RESPONSE OF BRIDGE ABUTMENTS TO BACKFILLING AND CRANE LOADING DURING CONSTRUCTION

FINAL REPORT

ODOT Task Order Number 2160-21-02

Submitted to:
Office of Research and Implementation
Oklahoma Department of Transportation

Submitted by:
Gerald A. Miller, Ph.D., P.E.
Tommy D. Bounds, Ph.D., P.E.
Kanthasamy K. Muraleetharan, Ph.D., P.E., G.E.

School of Civil Engineering and Environmental Science (CEES)
The University of Oklahoma

October 2021

Table of Contents

1.0 Introduction

During the construction of a bridge the placement of heavy equipment such as cranes is often restricted. Ideally cranes would be located at the bottom of the embankment during the placement of the bridge girders. However, obstructions such as existing roads, highways, and powerlines make this placement unfeasible some of the time. The next best place for the crane would be the bridge abutment backfill. However, the most common backfill used in bridge construction in the State of Oklahoma comes with placement restrictions. Controlled Low Strength Material (CLSM) is placed as a flowable mixture and puts fluid pressure on the abutments. The Oklahoma Department of Transportation (ODOT) has put construction sequencing restrictions in place to negate any negative effects of the CLSM placement. The restrictions state that the bridge superstructure must be in place before CLSM backfill can be placed. The rationale is that the superstructure is needed to counteract the pressure from the fluid CLSM. The restriction on CLSM placement limits the areas where the crane can be placed to set the girders.

Bridge contractors would like to construct the abutment and then place the CLSM backfill once the abutment concrete reaches the minimum acceptable strength. The backfill could then be used as a working pad to set the girders. Another benefit may be realized from this sequencing. Currently the abutment backfill cavity is left open during the superstructure placement. During this time the cavity can fill with water and sediment, plugging the drainage system and wetting the underlying fill.

A numerical investigation has been completed to study the placement of fluid CLSM which would later be used as a working pad for a crane. The numerical study was

completed using ANSYS® Mechanical, 2021 R1 (ANSYS 2021). A total of 135 analyses were completed for the parametric study. Variables such as abutment design, embankment soil strength and compressibility, crane position, and crane loading were systematically varied for the investigation. The simulations include the influence of fluid CLSM during placement as well as cured or solid CLSM under crane loading. A limited study was also completed to study the impact of granular backfill placement on the bridge abutment. The scope of the granular backfill analysis was limited and only nine analyses were completed. The worst-case scenario crane loading and placement was used for the granular fill analysis.

2.0 Background

While there are publications that address development of earth pressures during placement of granular backfill (e.g. Duncan and Seed 1986, Das and Sivakugan 2019), a review of the literature revealed very few publications that address development of backfill pressures on abutments due to CLSM placement or subsequent crane loading. There are numerous publications that address various aspects of CLSM as an abutment backfill such as for minimizing approach slab settlement and earth pressures during curing (e.g. Snethen and Benson 1998, Wilson 1999) and CLSM properties (e.g. Pons et al. 1998, Alizadeh et al. 2015, Alizadeh 2019), which provide some insight into the material behavior under cured conditions. There are some papers that address lateral displacements, particularly under seismic loading (e.g. Shamsabadi et al. 2010a, Shamsabadi et al. 2010b). There are also some papers that address using CLSM to construct innovative bridge abutments (e.g. Alizadeh et al. 2014b). While these publications provide some insight into modeling techniques and properties of cured CLSM, they don't directly address the pressures exerted by fluid CLSM during construction or subsequent construction loading from cranes with respect to the abutment lateral displacements.

Two publications that provide some insight into the pressures exerted by liquid CLSM are the Pennsylvania Department of Transportation Report on "CLSM Backfills for Bridge Abutments" (Newman et al. 1993) and the Kansas Department of Transportation report on "Use of Controlled Low-Strength Material as Abutment Backfill" (Schmitz et al. 2004). The are two significant findings reported by Newman et al. (1993) regarding the CLSM fluid pressures. First, fluid pressures exerted by liquid CLSM during

construction were approximately equal to the CLSM unit weight times the depth to the pressure cell. Second, fluid pressures developed on pressure gages at a lower point in the abutment corresponding to CLSM lift 2 experienced pressure increases during subsequent CLSM lifts 3 and 4, consistent with the height of the CLSM above the pressure gage. During lift 5, the recorded pressure dropped to low values indicating that liquid CLSM did not reach the pressure gage location. Apparently, the pressure on the abutment during lifts 3 and 4, combined with the shrinkage of the cured lift was enough to open a gap allowing the CLSM pressure to be exerted on lower portions of the wall. By lift 5, this gap was apparently closed. The CLSM was allowed to cure overnight between lifts. Work by Schmitz et al. (2004) using an instrumented model box in the laboratory confirmed that fluid pressures exerted by CLSM are approximately equal to the CLSM unit weight multiplied by the depth.

There are some important takeaways from the literature review regarding the modeling presented in this report. First, the CLSM acts like a fluid exerting a hydrostatic pressure distribution calculated using the unit weight of CLSM multiplied by depth. And second, in a worst-case situation, CLSM pressure may be exerted over the full wall height due to gapping between lower cured CLSM lifts and the abutment.

3.0 Numerical Modeling and Parametric Analysis

3.1 Finite Element Software

ANSYS 2021 R1 was used for the finite element modeling in this project. ANSYS can model a wide range of materials and systems in either two or three dimensions. The software includes material models and properties for many common materials. The materials library was utilized where possible for this research. All the analyses were 3D to capture the varying shape of the abutment and embankment. The element types used to model each component of the system are included below. The element types were automatically chosen by ANSYS based on the model setup.

3.2 Material and Model Parameters

This section presents the various components of the 3D model and the material models used to characterize the components within the model. The model included the abutment, abutment piles, embankment, and abutment backfill. The materials models used in these analyses were available within ANSYS.

3.2.1 Abutment

The abutment concrete was characterized using a linear elastic model. A Young's Modulus of approximately 4,350 ksi and a Poisson's Ratio of 0.18 were used for the concrete abutment. The material model and values are borrowed from the engineering materials library preloaded in ANSYS. The rebar in the abutment was not included in the model. HEX20 (20 nodes hexahedron) elements were used to model the abutment in ANSYS.

3.2.2 Piles

The bridge piles were characterized as structural steel using a linear elastic model. The model also incorporated the yield strength of the steel in compression and tension. The parameters used to characterize the bridge piles are shown in Table 1. The material model and values are taken from the engineering materials library preloaded in ANSYS. TET10 (10 nodes tetrahedral) elements were used to model the piles in ANSYS. The bridge piles used in the analysis were HP 10x42, HP 12x53, and HP 14x73.

Table 1. Pile Material Properties

Property	Value
Youngs Modulus (ksi)	29000
Poisson's Ratio	0.3
Tensile yield strength (ksi)	36
Compressive yield strength (ksi)	36

3.2.3 Embankment Soil

The embankment soil was characterized using the Cam-Clay model (Schofield and Wroth 1968). The model is elastoplastic which simulates the behavior of soil more realistically than a linear elastic model. In ANSYS the model requires six parameters to characterize a soil. The defined parameters and values assigned are shown in Table 2. Three soils were used during the simulations. The soils were chosen to represent varying soil stiffnesses. The soils are labeled as 1, 2, and 3. Soil 3 has the stiffest behavior while soil 1 has the softest behavior. The actual embankment stiffness properties can vary greatly throughout the state. An initial analysis was completed to

determine the softest soil which did not result in failure. Soil 1 represents the lower end of possible soil stiffness for which the simulation was able to run to completion. HEX20 (20 nodes hexahedron) elements were used to model the embankment in ANSYS.

Table 2. Embankment Soil Properties

Property	Soil 1	Soil 2	Soil 3
Slope of isotropic consolidation line in e – ln p' plot, λ	0.1	0.05	0.01
Slope of elastic rebound line in e – ln p' plot, κ	0.02	0.005	0.001
Slope of critical state line in q – p' space, M	1.24	1.24	1.24
Poisson's ratio, v	0.28	0.28	0.28
Void ratio, e	0.5	0.5	0.5
Initial size of the yield surface, p'_0 (psf)	1500	3000	6000

Note: p' and q are stress state variables in triaxial space, where $p' = (\sigma'_1 + 2\sigma'_3)/3$, $q = \sigma'_1 - \sigma'_3$, and σ'_1 and σ'_3 are the principle effective stresses.

3.2.3 CLSM Backfill

The CLSM backfill was characterized using the Mohr-Coulomb model. The model is a linear elastic - perfectly plastic model. Linear elastic parameters as well as parameters to define the yield surface are required to characterize the CLSM. The parameters used in the analysis are shown in Table 3. The parameters in the Table are representative of the cured CLSM. HEX20 (20 nodes hexahedron) elements were used to model the CLSM backfill in ANSYS.

Table 2. CLSM Backfill Properties

Property	Value
Young's Modulus (ksi)	1700
Poisson's Ratio	0.2
Cohesion (psf)	2900
Friction Angle (deg.)	45

A series of unconfined compression tests were completed with CLSM samples to determine the model parameters of the CLSM. The CLSM samples were gathered by the ODOT Oklahoma City Residency and transferred to the University of Oklahoma on April 9, 2021. Nine standard 4 x 8 inch samples were collected. The samples were tested after 7, 14, and 28-day curing intervals. The samples gained strength rapidly before leveling off between 7 and 14 days of curing time. The results of the unconfined compression tests are shown in Figure 1. It should be noted that some of the 14 and 28 day samples were not tested to failure due to testing device limitations.

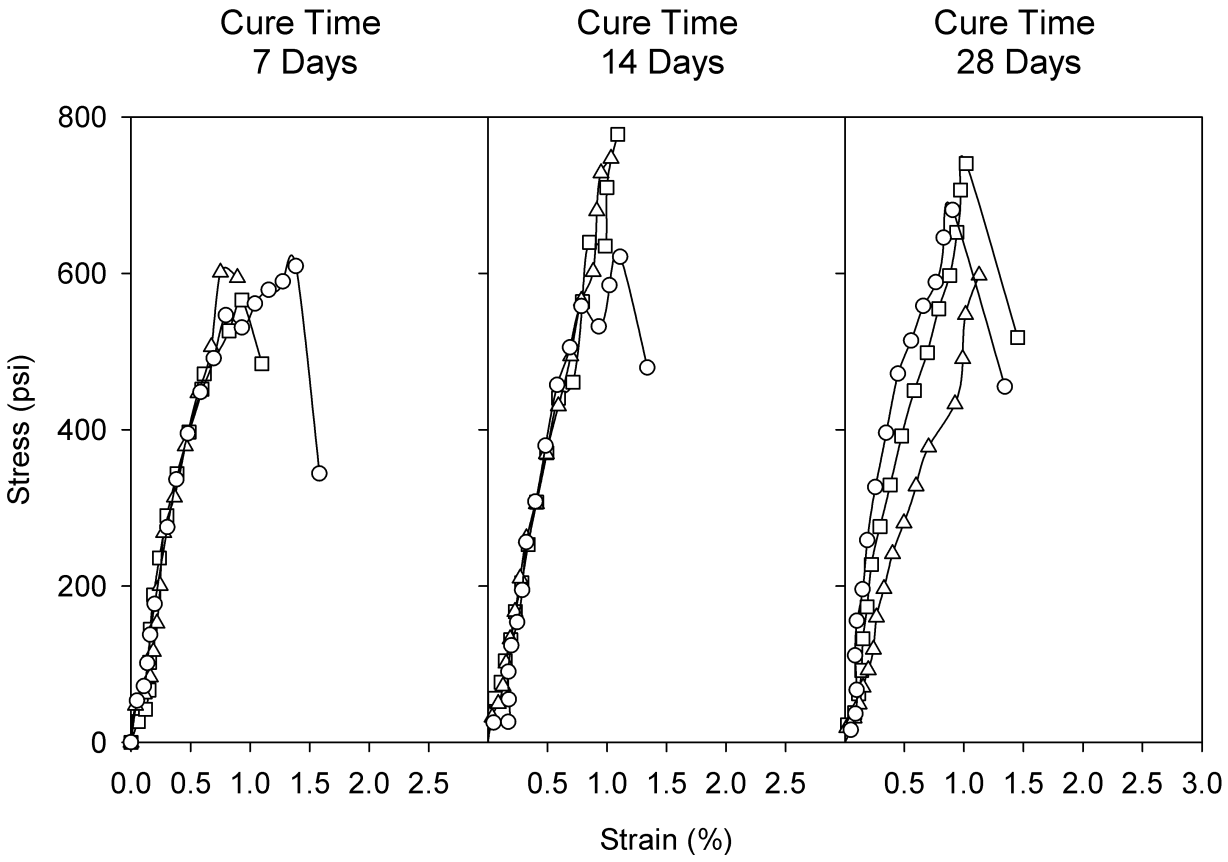

Figure 1. CLSM Field Samples – Unconfined Compression Results

The results of the 14 and 28 day samples were used to calibrate the Mohr-Coulomb model. A comparison between a simulated unconfined compression test and a set of recorded test results is shown in Figure 2.

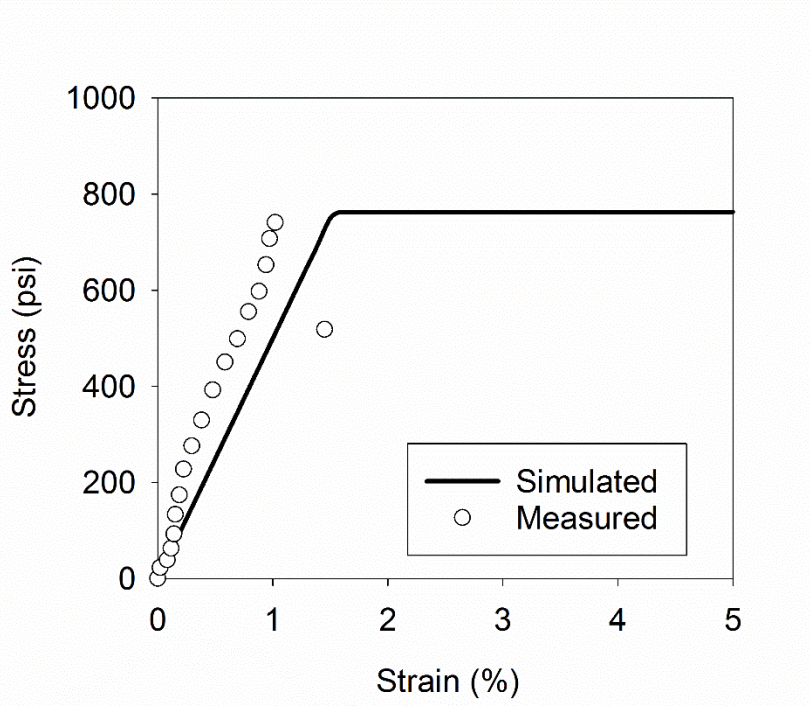

Figure 2. Mohr-Coulomb CLSM Predictions

The effects of fluid CLSM placement on the abutment are of interest for this research. To capture the effect of fluid CLSM placement, a hydrostatic pressure was applied to the inside walls of the abutment and wingwalls during this stage of the loading. The hydrostatic pressure represented a fluid with a unit weight of 120 pcf. The hydrostatic pressure was later turned off and replaced with solid CLSM backfill to simulate the cured CLSM during subsequent crane loading.

3.2.3 Granular Backfill

Granular backfill was also considered in the study. The simulations involving granular backfill are not as comprehensive as those involving CLSM. Instead, only the

impacts of granular backfill compaction and the worst-case scenario with regard to crane loading is considered. The granular backfill was characterized using the Mohr-Coulomb model. The parameters used in the analysis are shown in Table 4. HEX20 (20 nodes hexahedron) elements were used to model the granular backfill in ANSYS.

Table 4. Granular Backfill Properties

Property	Value
Young's Modulus (ksi)	5.5
Poisson's Ratio	0.25
Cohesion (psf)	0
Friction Angle (deg.)	40

It is common in Oklahoma to place granular backfill in large lifts and densify it by flooding the backfill while the drainage outlets are temporarily blocked and using a concrete vibrator to densify the soil. This results in both an active earth pressure component and hydrostatic water component acting against the abutment during construction. Because this technique involves significant hydrostatic loading due to temporary flooding it was used for the analysis presented.

3.3 Abutment and Embankment Geometry

Three abutment designs were analyzed in the simulations. Due to symmetry, only half of the abutment, embankment, and crane tracks were modeled. The computational effort was reduced by taking advantage of the symmetry about the centerline of the abutment. This was done to evaluate the influence that backwall height has on the behavior of the abutment during the simulated loading. Two of the abutments were stub type abutments and the remaining abutment was a full height abutment. The

shortest abutment was based on ODOT Type III abutment details (B40-C-ABUT-PC3). A plan view and typical section of the bridge seat is shown in Figure 3. The Type III abutment as modeled is shown in Figure 4. The mid height abutment was based on ODOT Type J abutment details (B40-C-ABUT-PC5). A plan view and typical section of the bridge seat is shown in Figure 5. The Type J abutment as modeled is shown in Figure 6. Standard details are not available for the full height abutment. The simulations were based on the Main Street over I-35 in Norman, OK as built plans provided by ODOT. Main Street over I-35 in Norman has ODOT JP number 09031(08). A typical section view is shown in Figure 7. The full height abutment as modeled is shown in Figure 8. The full height abutment varies in height along the length of the abutment. The tallest abutment section was modeled for the simulations.

The two stub abutments were modeled with the wingwall as one piece. Only a section of the full height abutment was modeled. This was done due to the length of the abutment. The abutment is approximately 285 ft long. The effects of a crane near the middle of the abutment would not be felt at the edges. The full height abutment did not have wing walls so the interactions between the wingwall and abutment were not a concern. A retaining wall begins at the end of the full height abutment. The full height abutment was separated into 4 ft tall segments. This was done so that the effects of fluid CLSM could be properly modeled. The CLSM was placed as a single lift for the two stub abutments and was placed in 4 ft layers for the full height abutment. The single lift would represent a worst-case scenario but the movement for the full height abutment was very large when a single CLSM layer was considered. This observation suggests that CLSM placement for full height abutments may not be viable, without abutment

lateral support. The reason is that there exists the possibility that full CLSM fluid pressure could develop over a large portion of the abutment height if a gap forms between the abutment and lower cured CLSM lifts.

The connection between the piles and the abutment is treated as a fixed connection. To ensure a rigid connection, a steel plate was attached to the top of the piles. The steel plate is then bonded to the abutment. In the model the piles do not extend into the abutment.

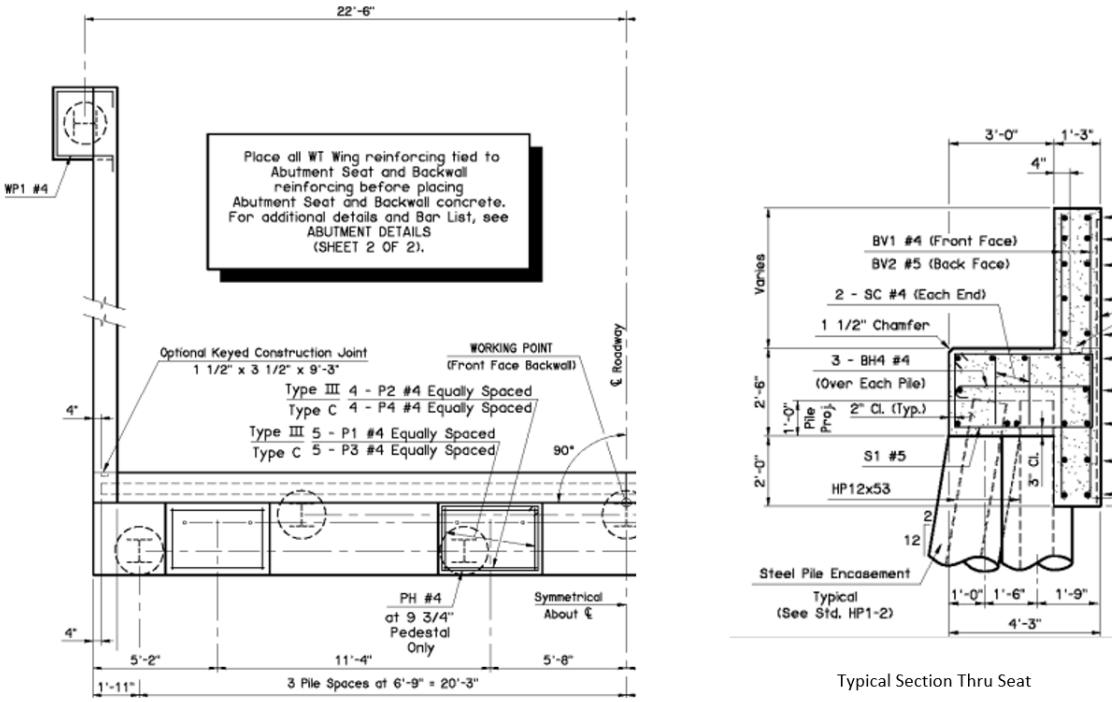

Figure 3. Type III Detail; ODOT 2009 Standard Specifications

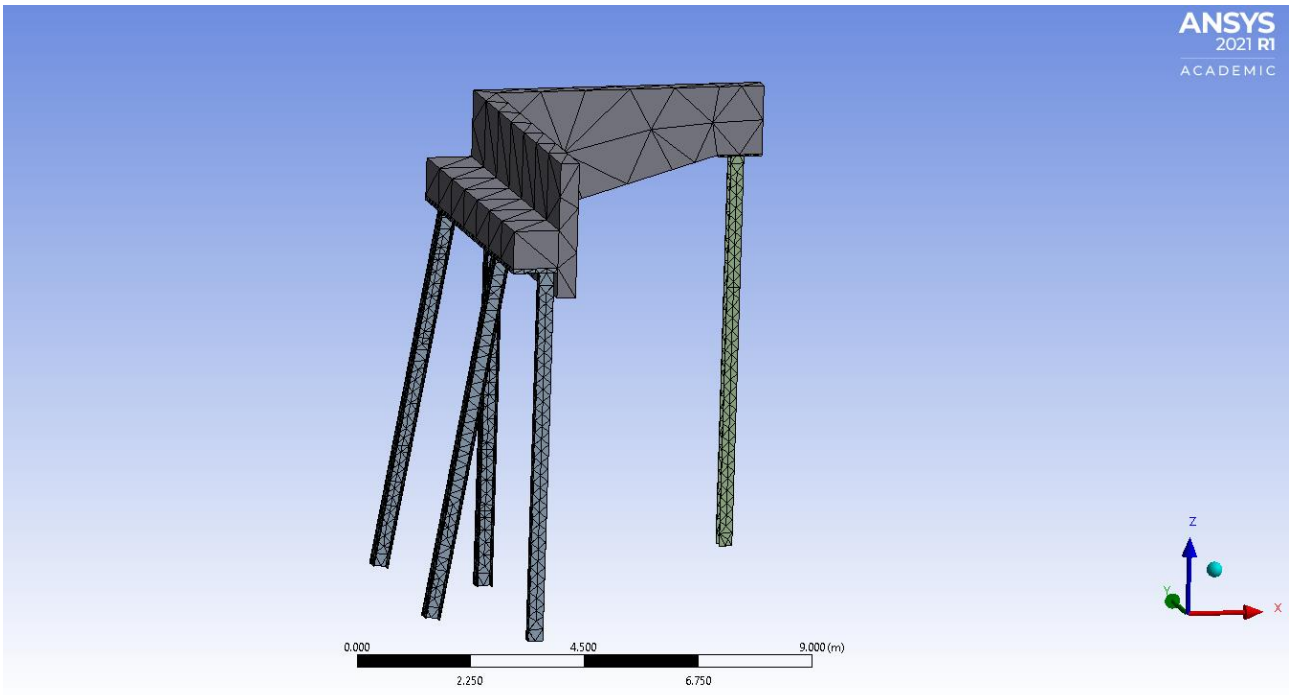

Figure 4. Type III Abutment and Piles - Model and Mesh

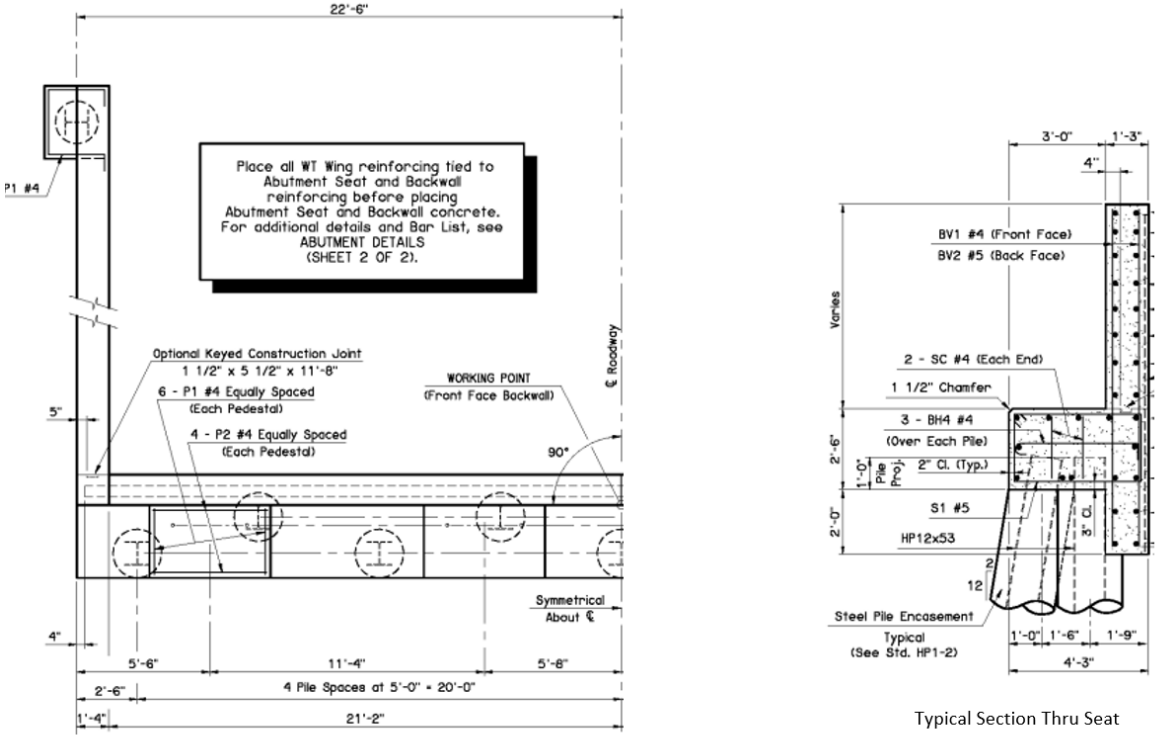

Figure 5. Type J Detail; ODOT 2009 Standard Specification

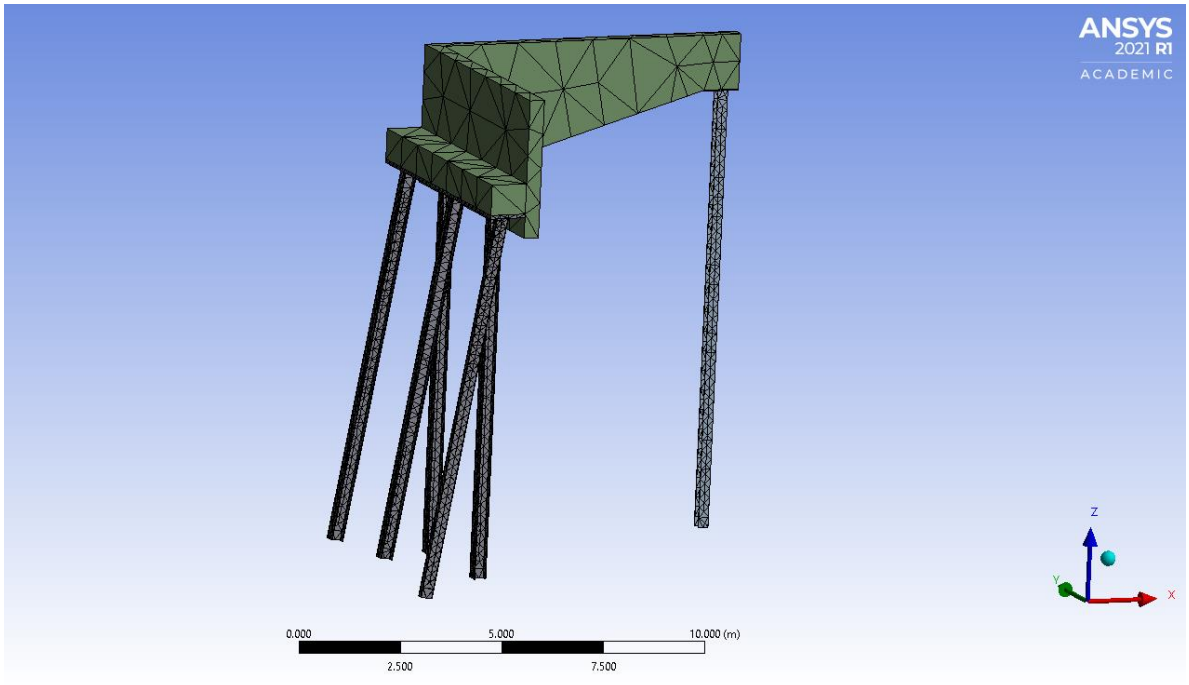

Figure 6. Type J Abutment and Piles - Model and Mesh

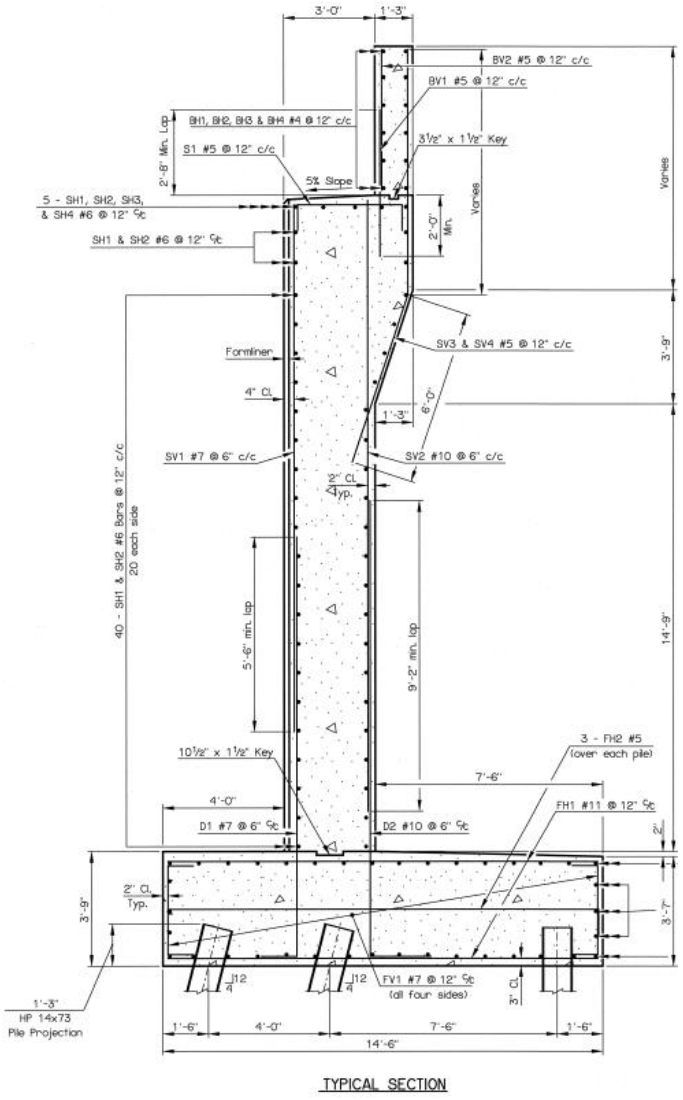

Figure 7. Full Height Abutment Detail; Main Street over I-35 in Norman, OK

ODOT JP# 09031(08)

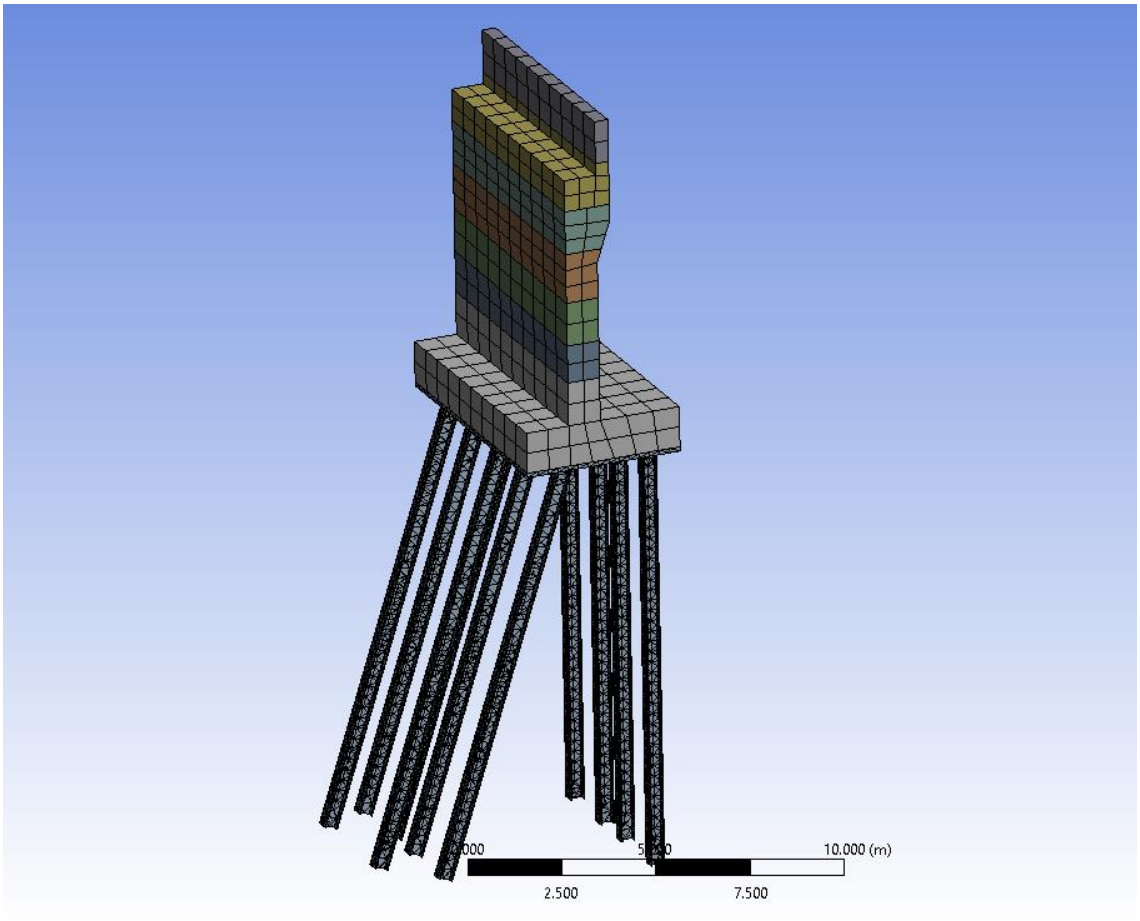

Figure 8. Full Height Abutment and Piles - Model and Mesh

The embankments used in the two stub abutment models had side and foreslopes of 3H:1V. The embankment extended 11 ft below the bottom of the Type 3 stub abutment and 20 ft below the Type J stub abutment. The embankment used in the full height abutment was based on the plans for Main Street over I-35 in Norman. The embankment extended 15 ft below the full height abutment. The height of the embankment was optimized prior to the parametric study. To do this various embankment heights were investigated to determine the depth of influence for each embankment configuration. The optimization was necessary to reduce computational effort. The piles were extended approximately 10 feet below the embankment to

simulate the soil-structure interaction of the piles with the embankment foundation soils. A linear elastic soil pressure was applied to the horizontal face of the piles to simulate the soil response below the embankment. The horizontal pressure was equivalent to a soil reaction of 50 pci. This soil reaction would be representative of a soft soil. The pile length, foundation soil behavior, and soil reaction, can vary greatly throughout the state. These two variables were not the focus of this study so they were kept constant throughout the analysis.

The embankment geometry and mesh for the Type III abutment, Type J abutment, and full height abutment are shown in Figures 9, 10, and 11. The Type III abutment model contained 13,904 elements and 32,912 nodes. The Type J abutment model contained 23,375 elements and 54,214 nodes. The full height abutment contained 33,208 elements and 91,809 nodes. The piles contained the highest element density. The high element density was necessary to fully capture the flanges and webs of the piles.

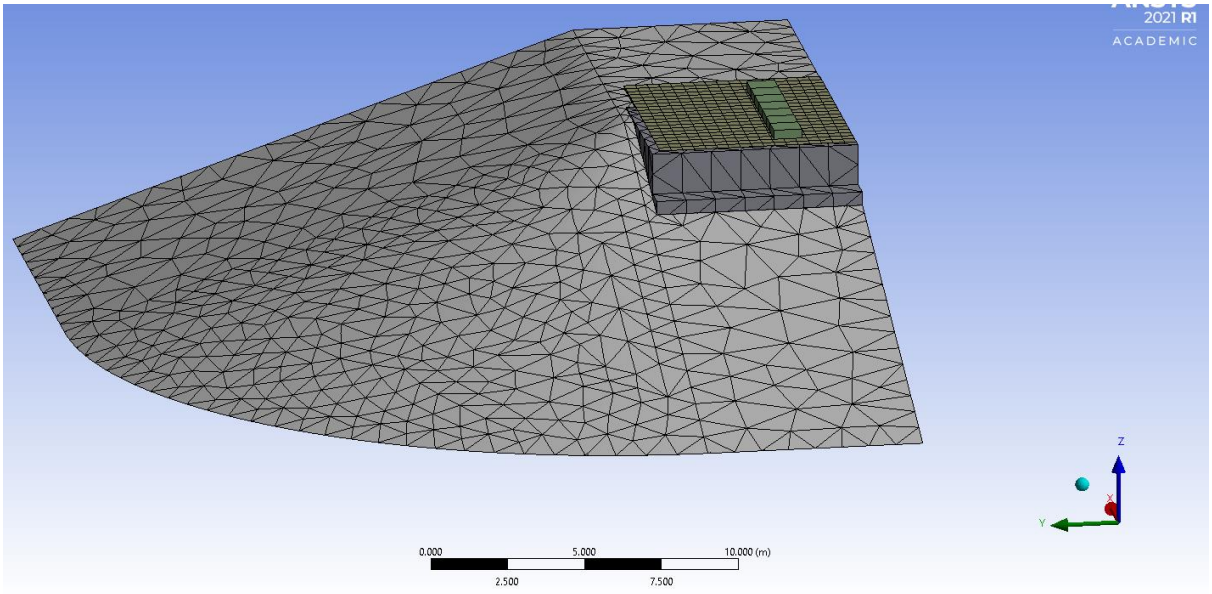

Figure 9. Type III Embankment - Model and Mesh

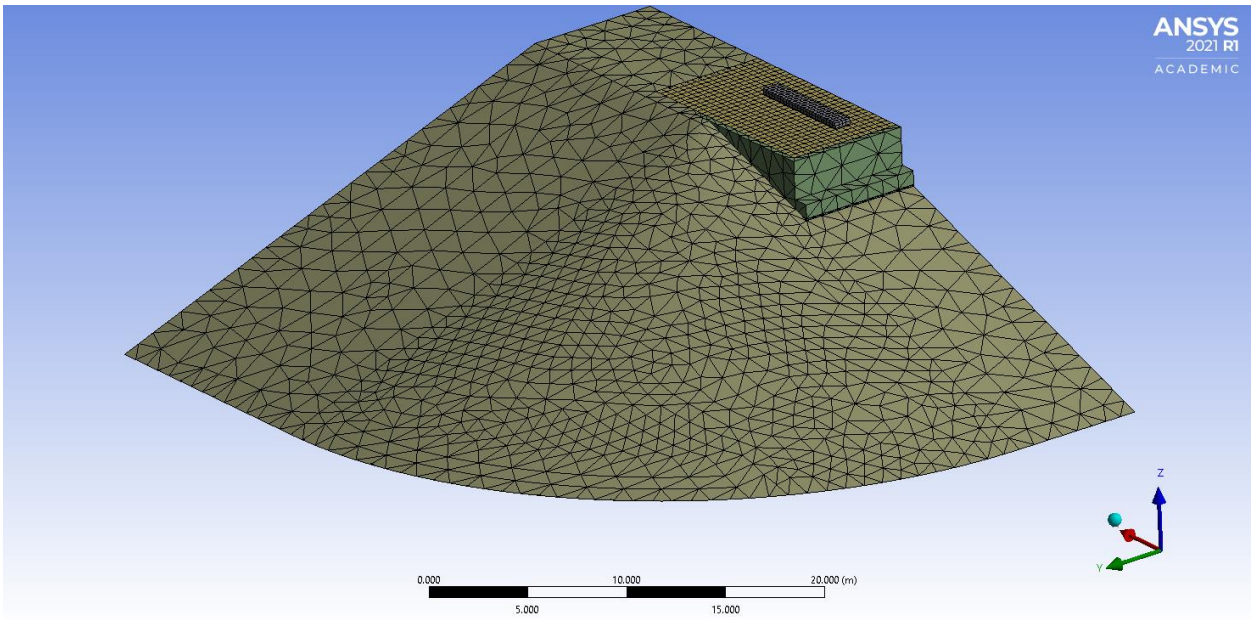

Figure 10. Type J Embankment - Model and Mesh

Horizontal and vertical displacements were held at zero along the bottom boundary of the Type III and Type J embankment model. Horizontal displacements were held at zero along the two truncated sides of the embankment. Horizontal and vertical displacements were held at zero at the pile tips.

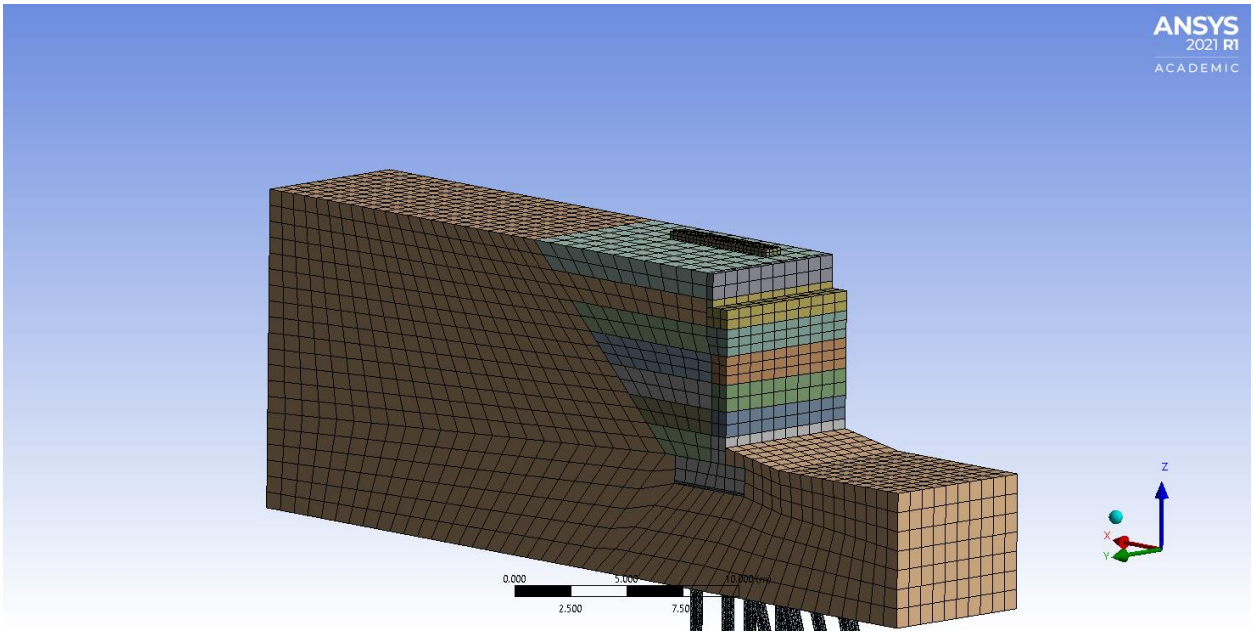

Figure 11. Full Height Abutment - Model and Mesh

Horizontal and vertical displacements were held at zero along the bottom boundary of the full height embankment model. Horizontal displacements were held at zero along the three truncated sides of the embankment. Horizontal and vertical displacements were held at zero at the pile tips.

Within ANSYS the connections between the various parts must be defined. The connection between the abutment and the piles was bonded. A bonded connection means sliding and gapping between the objects is not allowed. Sliding and gapping were allowed between the piles and the embankment soil. Sliding was allowed between the abutment and the embankment, but gaps were not allowed to form. Sliding was allowed between the backfill and the embankment, but gaps were not allowed to form. Sliding was allowed between the backfill and the abutment but gapping was restricted for the stub abutments. In the full height abutment analyses, gapping and sliding were allowed between the abutment and the backfill. During these analyses the backfill moved toward the abutment so gapping between the backfill and abutment was not an issue. Gaps were allowed to form between the full height abutment and the backfill. As will be discussed in the results section, the backfill rotated away from the abutment for some of the analyses. If a gap could not form the backfill would have pulled the abutment with it as it settled and rotated, which would have been physically unrealistic.

3.4 Load Placement and Sequence

The following section presents the sequencing for the placement of CLSM backfill, granular backfill, and crane placement and loading.

3.4.1 CLSM Backfill

For the stub type abutments, the CLSM was initially modeled as a hydrostatic pressure on the inside walls of the abutment. This was done to model the effect of fluid CLSM on the abutment. The hydrostatic pressure was then turned off within the model. The solid CLSM was turned on during the same step that the hydrostatic pressure was turned off. A similar loading pattern was followed for the full height abutment. Since the full height abutment CLSM was placed in 4 ft lifts the process of fluid and cured CLSM placement was repeated for each lift. The models used in this analysis are not time dependent. Furthermore, the solid elements used to model the embankment soil did not consider excess pore water pressures or have a permeability assigned to them. The loading sequence for the stub type and full height abutments are shown in Figures 12 and 13. Phases 5 through 11 have been omitted from the full height abutment loading sequence figure. The omitted phases follow the same process as phases 3 and 4. That is the fluid CLSM load is placed on the abutment and then the solid CLSM is placed as the fluid CLSM load is turned off. Note that the CLSM loading in the full height abutment assumes that a gap does not form between the solid CLSM and abutment in the lifts underlying the fluid CLSM.

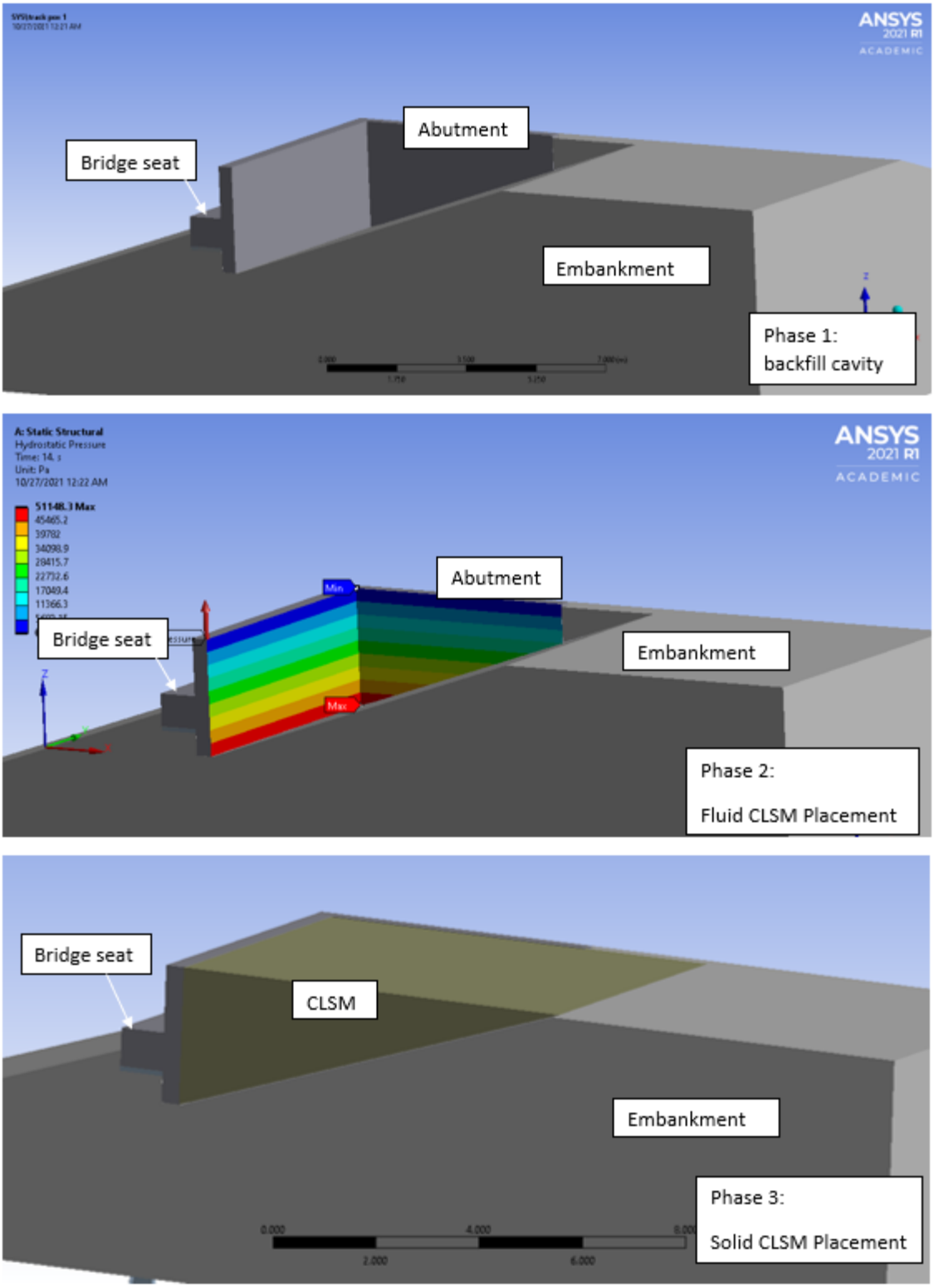

Figure 12. Stub Abutment - CLSM Placement

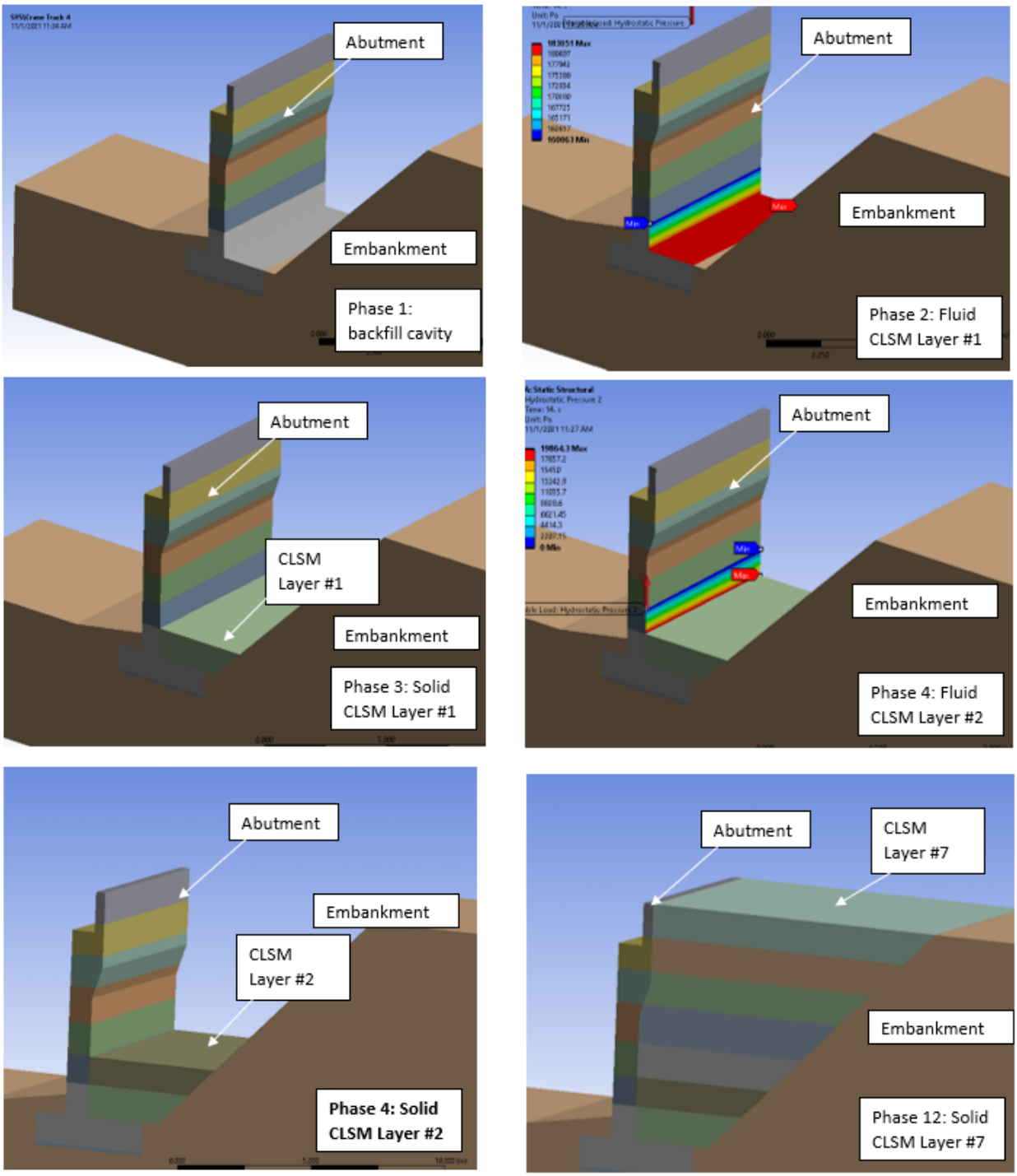

Figure 13. Full Height Abutment - CLSM Placement

3.4.2 Granular Backfill

For the stub type abutments, the granular backfill was placed in the backfill cavity in 4 ft lifts. The lateral pressure from placement of the granular backfill was applied to

the backwall and wingwall using a linearly varying pressure. The lateral pressure represented the at rest earth pressure from the backfill. An at rest earth pressure coefficient of 0.5 was assumed for the analysis. The abutment cavity was then flooded. The flooding was simulated by applying a hydrostatic water pressure to the backwall and wingwall. The hydrostatic pressure was applied to the full height of the backwall and wingwall to simulate a worst-case scenario. The hydrostatic pressure was then removed to simulate draining of the flood water. This process of granular backfill placement and flooding was continued until the backfill reached the top of the abutment.

3.4.3 Crane Loading

Several cranes were reviewed to determine the dimensions and loading of the cranes used in bridge construction within the state. Communication with local contractors revealed three common crane sizes used in the state. The cranes reviewed, in increasing size and load capacity, were the Terex HC 80, Terex HC 110, and the Manitowoc 14000. The three track pressures used to simulate the loading in the analysis were 2000, 3000, and 4000 psf. This represents a broad range of crane loads with a range of payloads. The crane track was modeled as a 3 x 20 ft rectangle. The crane track dimensions were typical of the smaller two cranes included in the review. The crane track dimensions and applied pressures represent a total crane plus payload of 240,000 to 480,000 lbs.

The location of the crane tracks with respect to the abutment was also varied. Five crane positions were analyzed. The crane positions were 1, 2.5, 4, 5.5, and 7 ft from the inside edge of the abutment backwall. The crane position perpendicular to the centerline of the abutment was not investigated. It was assumed that the crane would

remain stationary once in place for many of the bridges. During the analyses the crane was centered on the centerline of the abutment.

The crane track elements were turned on once all the solid CLSM was in place within the model. The pressure to the track representing the crane loading was then applied. Once applied, the track pressure was held constant for the remainder of the analysis.

4.0 Results of Numerical Modeling

A total of 144 analyses were completed. The embankment soil, abutment design, crane load and crane position were systematically varied for the analysis. The response of the abutment to the placement of fluid CLSM and granular backfill are presented first. The only results shown for this phase of the loading are the abutment displacements. Following this the response of the abutments to the crane loading are presented.

4.1 Response of Abutments to Backfilling

The following sections discuss the response of the abutments to the placement of CLSM backfill or granular backfill. The CLSM backfill is placed as a fluid and then exchanged for a solid. The granular backfill is placed using the flooding method. The deflections presented in the figures are representative of the maximum lateral movement the abutment experienced during or directly following the backfill placement.

4.1.1 CLSM Backfill

The maximum displacement responses of the abutments when fluid CLSM was placed are shown in Figure 14. The maximum deflection is taken at the top edge of the abutment. The figure presents the response for the three abutment designs and three embankment soils considered in these analyses. The embankment soils are presented on the horizontal axis. The soil stiffness is dependent upon the stress history of the soil so numerical values were not assigned to the soil stiffness. One on the horizontal axis represents the softest soil, soil 1, and three represents the stiffest soil, soil 3. The two stub abutments experienced similar trend with increasing soil stiffness. As the soil

stiffness increases the abutment experiences less movement. This is likely the result of higher pile resistance from the stiffer soil. The Type J stub abutment experienced the most movement. This can be attributed to the taller backwall. The soil stiffness had less of an impact on the full height abutment behavior. The full height abutment is a more complex system due to the CLSM being placed in layers. The values on the chart represent the largest displacement experienced during the series of CLSM backfill placements.

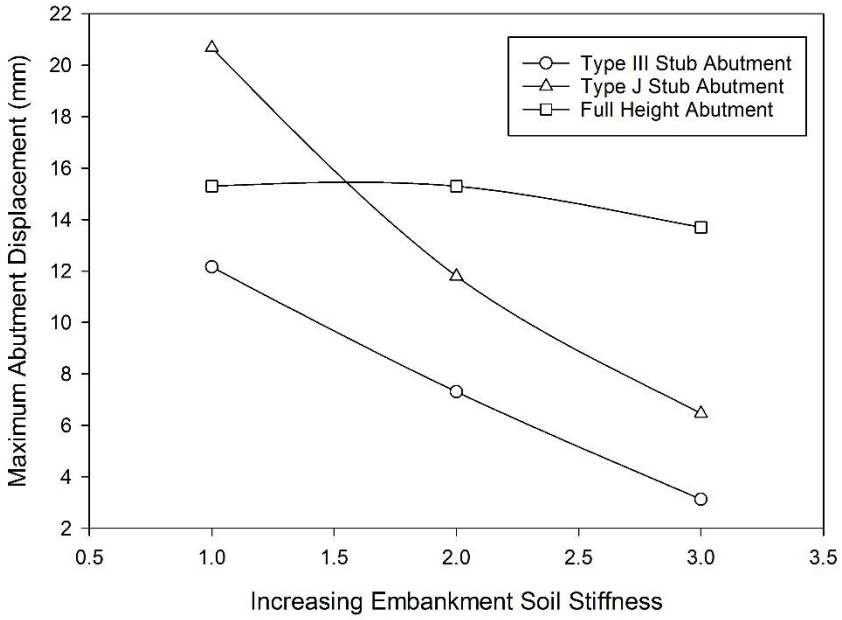

Figure 14. Abutment Displacements During CLSM Backfilling

4.1.2 Granular Backfill

The maximum displacement responses of the abutments when granular backfill was placed are shown in Figure 15. The two stub abutments experienced similar trends with increasing soil stiffness. As the soil stiffness increases the abutment experiences less movement. This is likely the result of higher pile resistance from the stiffer soil. The Type J stub abutment experienced the most movement. Soil stiffness also had an impact on the full height abutment when granular backfill is placed. The full height

abutment experienced much more movement than the stub abutments for these analyses. This is unlike the CLSM where each fluid lift in the full height abutment was turned to solid before the next fluid CLSM lift was placed. The solid CLSM exerts less pressure than granular backfill, which, unlike CLSM, exerts pressure over the full height of the wall during each lift.

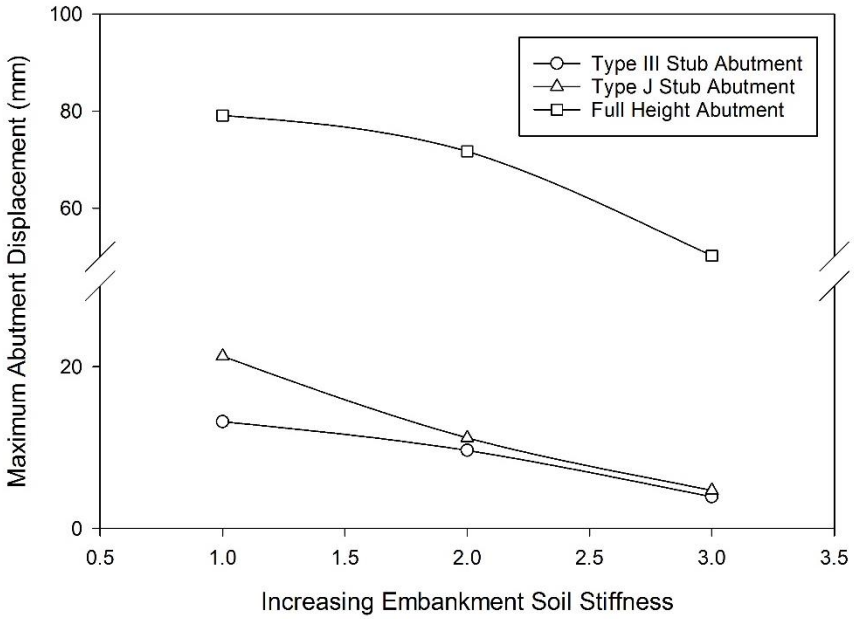

Figure 15. Abutment Displacements During Granular Backfilling

4.2 Response of Abutments to Crane Loading

The following sections discuss the response of the abutments to the placement of the crane and crane payload. The deflections presented in the figures are representative of the maximum lateral movement the abutment experienced once the crane and crane payload were placed on the backfill.

4.2.1 On CLSM

The maximum abutment displacements from the analysis for each of the three abutments are shown in Figures 16, 17, and 18. The crane position is included in the graphs and is indicated by the different symbols as shown in the chart legend. The distances in the legend are measured from the inside face of the abutment. As the crane load increased and the soil stiffness decreased the maximum abutment displacement increased for the two stub type abutments. The crane placement had a greater impact on the behavior of the abutment when the soil was weaker. This can be seen when considering Figure 17. Embankment soil 3 was affected very little with respect to the position of the crane. However, the abutment displacement for embankment soil 1 varied as much as 2 mm for the same crane load when the crane position was varied. The height of the stub abutment also had an impact on the influence of the crane position. This can be seen by comparing Figure 16 and 17.

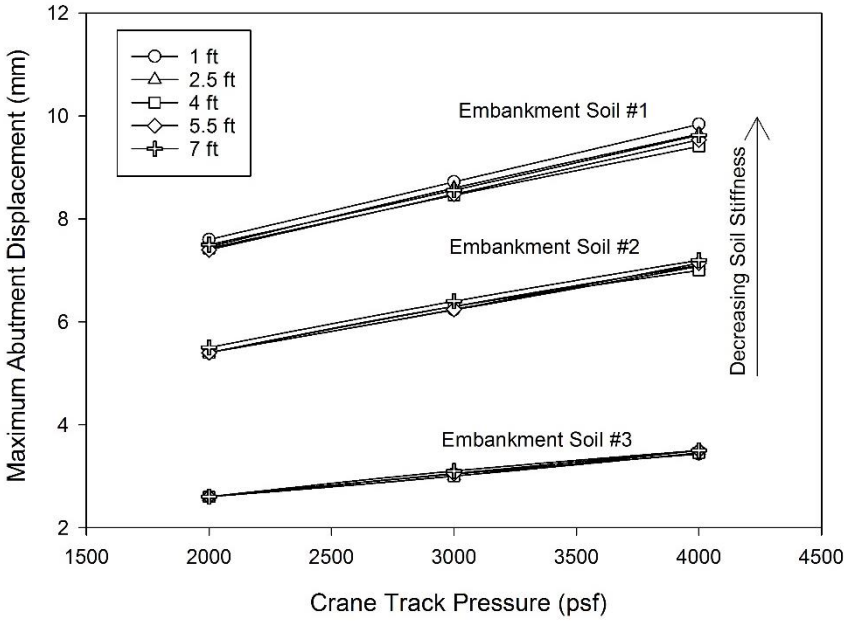

Figure 16. Type III Abutment – Abutment Displacements

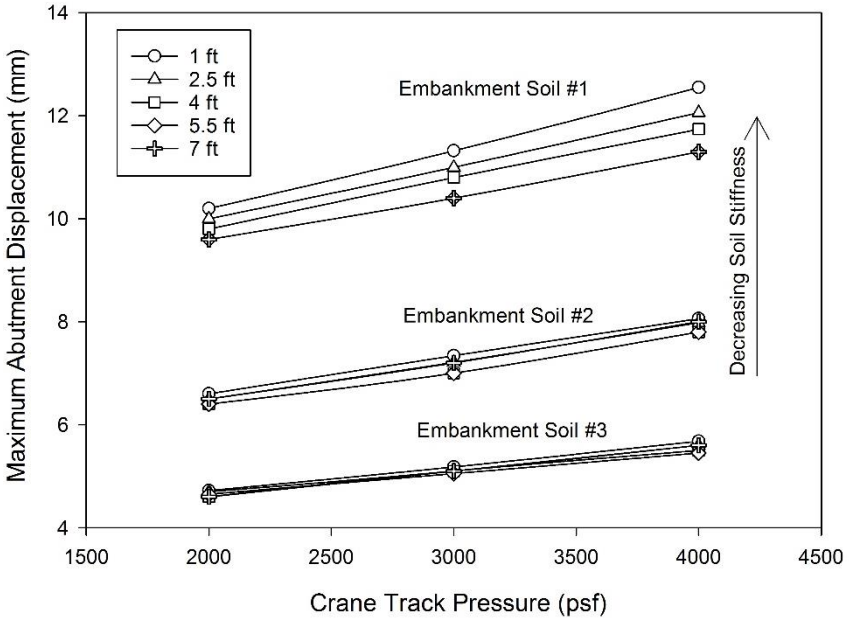

Figure 17. Type J Abutment - Abutment Displacements

The full height abutment, Figure 18, did not experience the same behavior as the stub type abutments. An opposite trend was found between soil stiffness and maximum displacement. Notice in Figure 18 that when the soil has low stiffness, embankment soil 1, the displacement is negative. A negative displacement indicates that the abutment was moving away from the bridge. When the soil has low stiffness there is settlement as the CLSM is placed. The settlement causes the CLSM to rotate away from the abutment. The abutment does experience a little movement in the same direction at the top. The full height abutment was essentially isolated from the impact of the crane loading since a gap formed between the abutment and backfill. An image of this behavior as captured in the finite element modeling is shown in Figure 19. The image is exaggerated by 10 times to emphasize the behavior. As the soil stiffness increased the gap between the abutment did not form. In these analyses the CLSM moved toward the

abutment. The magnitude of the crane loading and crane position had little impact on the magnitude of abutment displacement for the full height abutment.

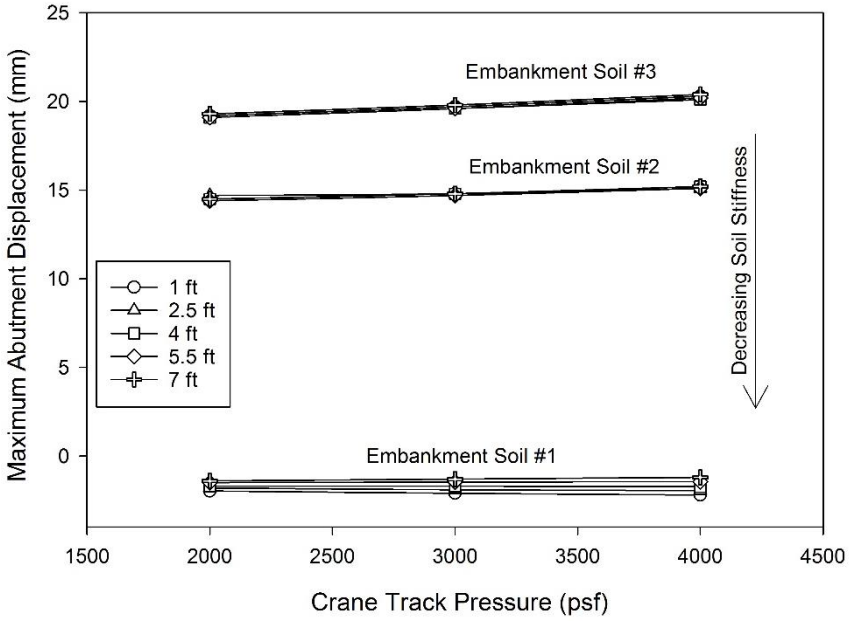

Figure 18. Full Height Abutment - Abutment Displacements

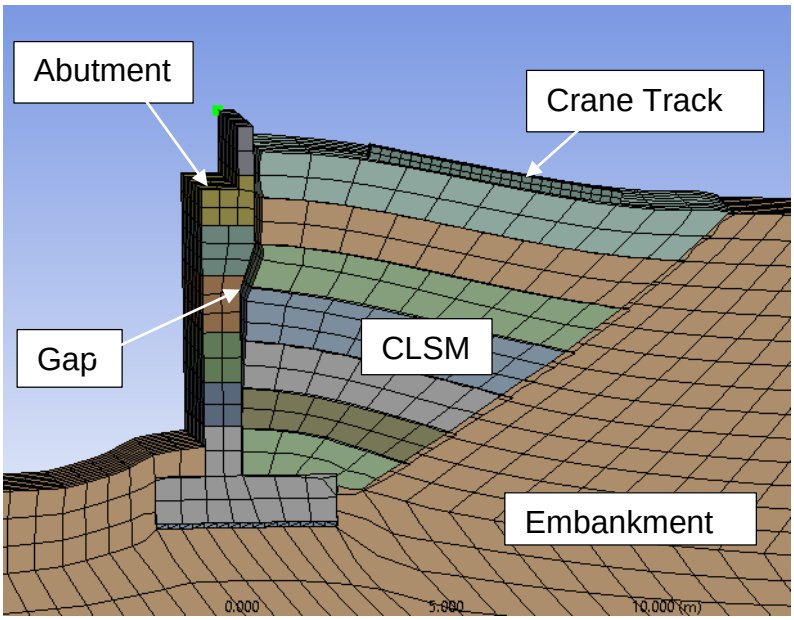

Figure 19. Full Height Abutment - Low Stiffness Embankment Soil

The maximum pile displacements from the analyses for the three abutments are shown in Figures 20, 21, and 22. The two stub abutments had a similar trend. As the crane load increased and the soil stiffness decreased the maximum pile displacement increased. The maximum abutment pile displacement for all analyses occurred at the connection with the abutment. The maximum pile displacements are similar to the maximum abutment displacements for the stub type abutments.

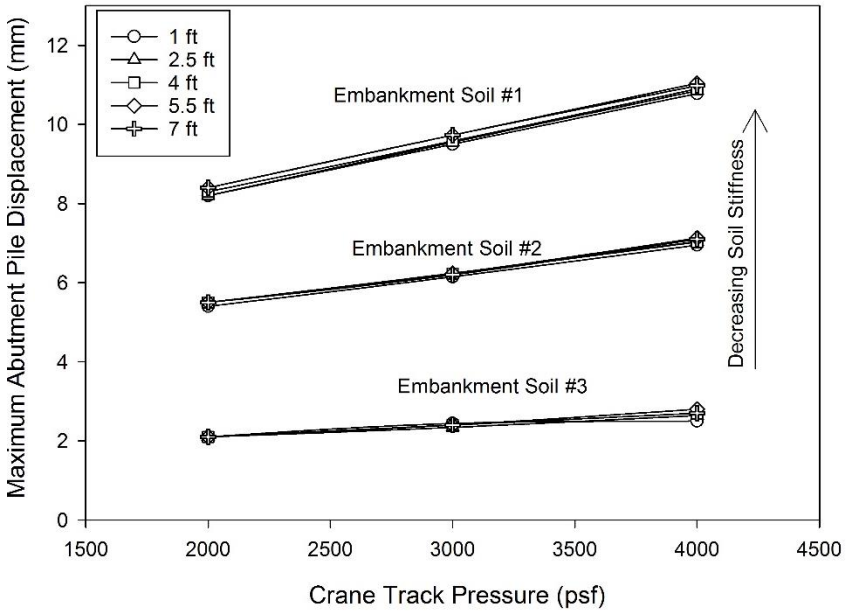

Figure 20. Type III Abutment - Pile Displacements

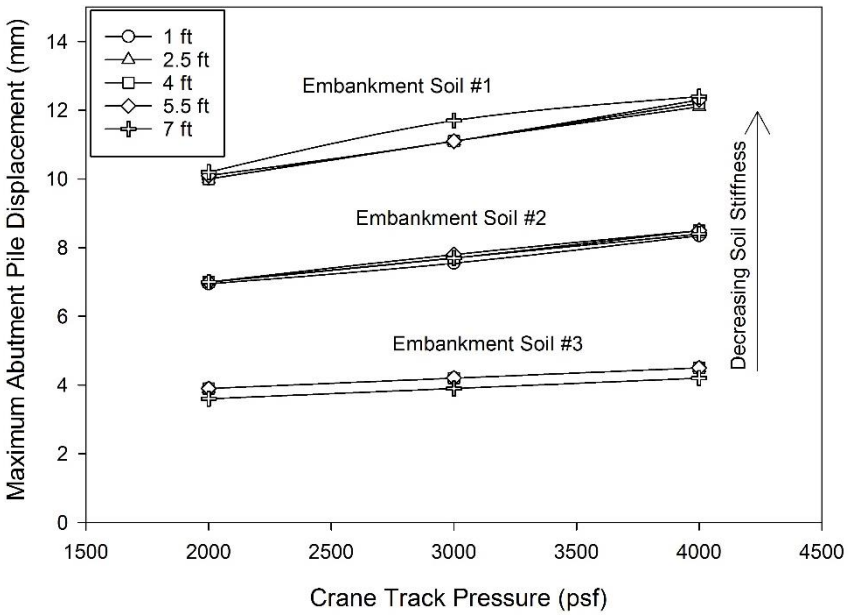

Figure 21. Type J Abutment - Pile Displacements

A similar trend was found for the full height abutment. The full height abutment displacement was less sensitive to changes in crane loading. The differences between the pile and abutment top displacement suggests tilting of the abutment. The piles for embankment soil 3 had an approximate displacement of 2 mm and the abutment experienced a displacement of approximately 20 mm.

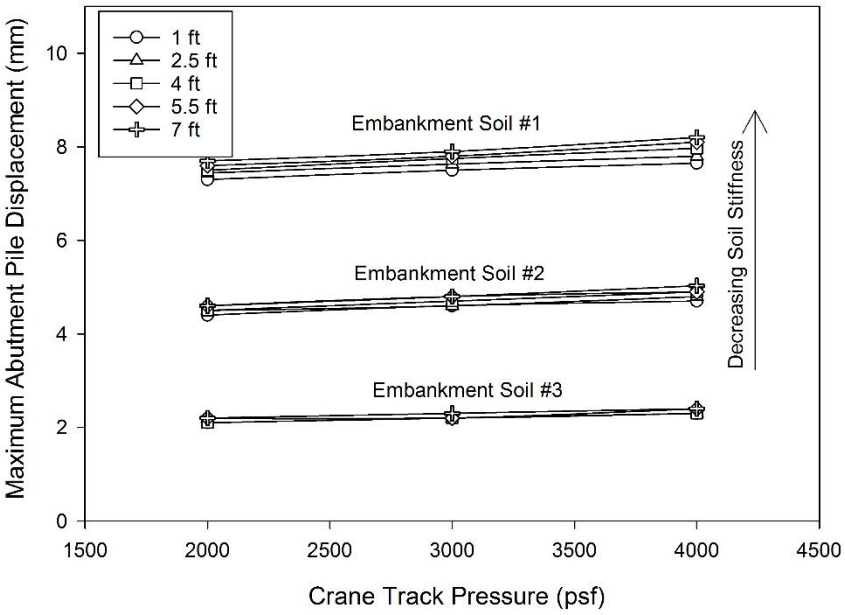

Figure 22. Full Height Abutment - Pile Displacements

The maximum vertical crane displacements from the analyses for the three abutments are shown in Figures 23, 24, and 25. All the abutments had a similar trend. As the crane load increased and the soil stiffness decreased the maximum vertical crane displacement increased. The maximum vertical displacement for each embankment soil occurred when the crane was furthest from the abutment. This is because at this position a portion of the crane track was often on the embankment soil which is weaker than the CLSM. Some of the estimated crane track displacements are large, however this likely would not be an issue since the crane is temporary. Any excessive crane track settlement could be remediated in the field. Note also that construction pads used under cranes would decrease the bearing pressure and reduce crane settlement. This may also have some effect on the abutment displacements.

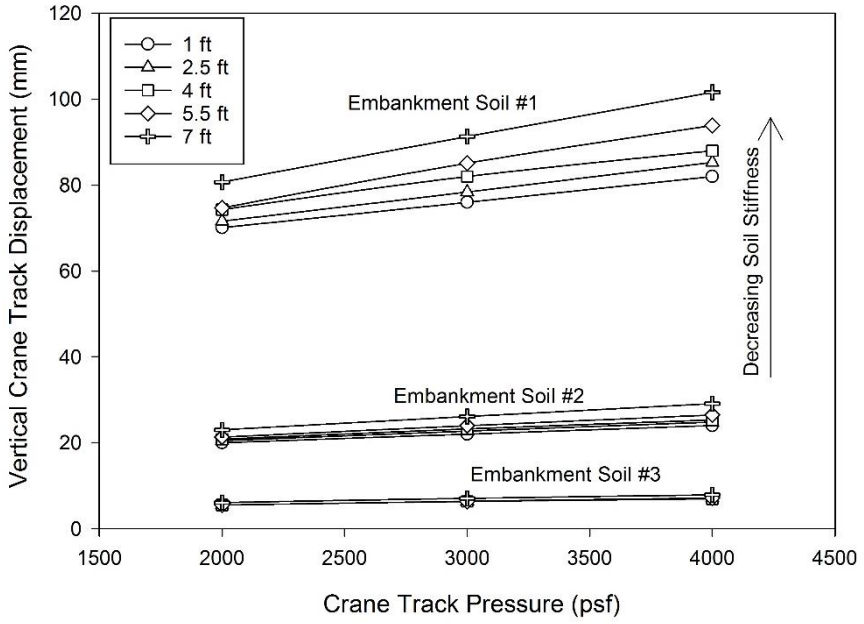

Figure 23. Type III Abutment - Crane Track Vertical Displacements

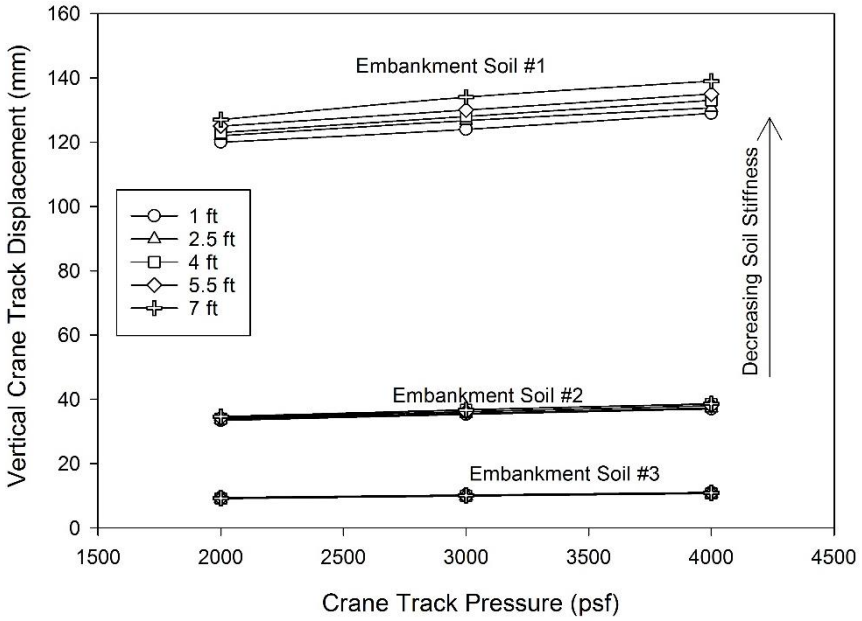

Figure 24. Type J Abutment - Crane Track Vertical Displacements

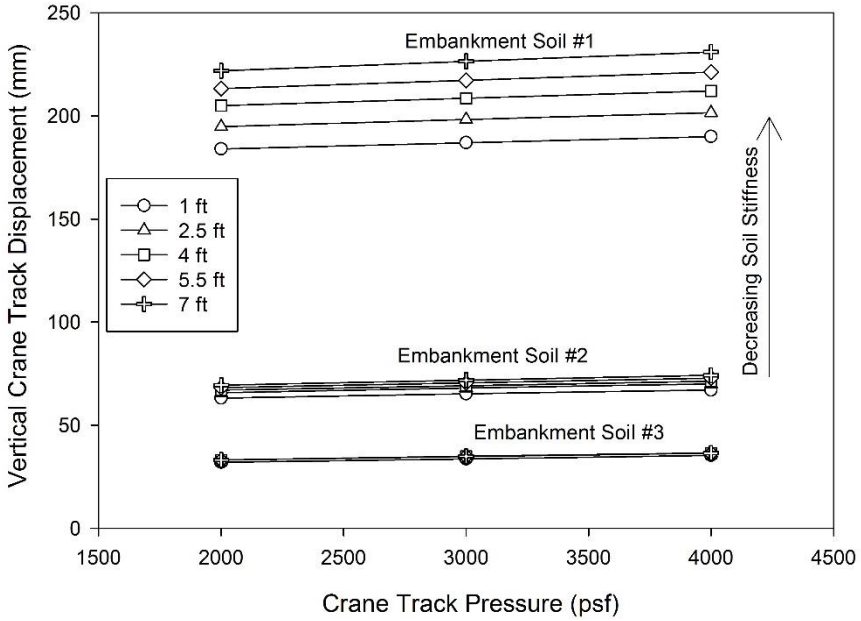

Figure 25. Full Height Abutment - Crane Track Vertical Displacement

The maximum abutment principal stresses from the analyses for the three abutments are shown in Figures 26, 27, and 29. The maximum principal stress for the stub type abutments increases as the soil stiffness decreases. The maximum principal stress was more sensitive when the soil stiffness is low. A positive principal stress in the model represents a tensile stress. The reinforcing rebars in the abutment would carry the majority of the tensile stresses in the abutment. The stub abutments are reinforced with #4 and #5 rebars. The full height abutment is reinforced with #5, #6, #7, and #10 rebars. The minimum yield stiffness of reinforcing steel allowed in the abutments is 60 ksi. Hence the minimum yield stress of a #4 bar (nominal area = 0.2 in^2) is approximately 12,000 psi which is much greater than the maximum values from the analysis.

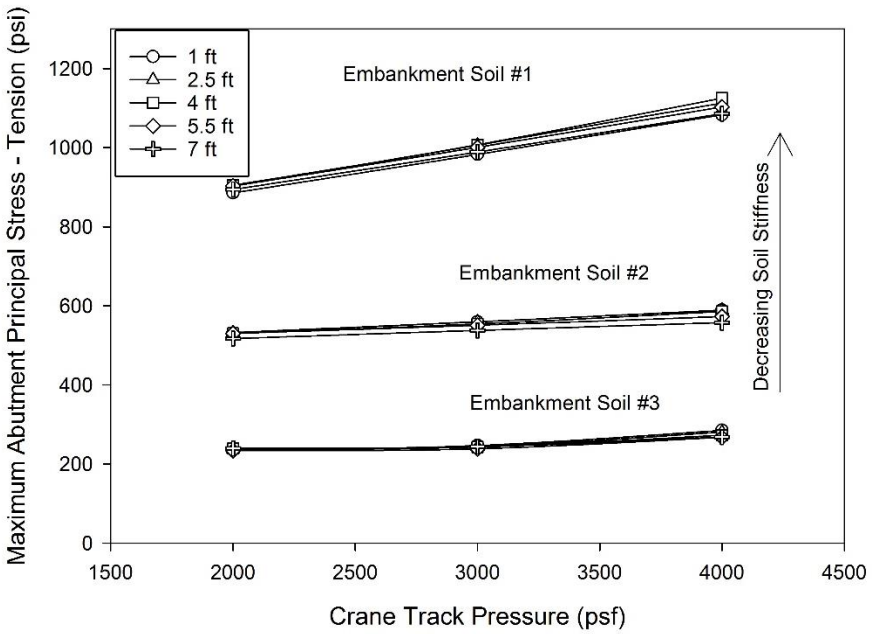

Figure 26. Type III Abutment - Maximum Principal Stress

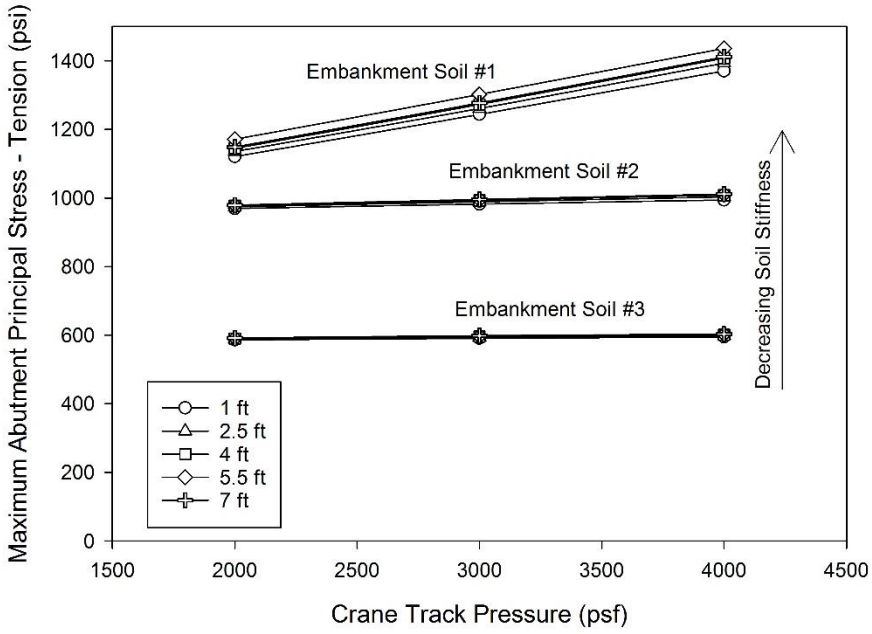

Figure 27. Type J Abutment - Maximum Principal Stresses

The maximum principal tensile stress occurred near the interface of the abutment and wingwall. The stress isochrones from one of the analyses are shown in Figure 28.

The red isochrones represent the maximum principal stress, which are tensile, and the blue represents the minimum principal stress, which is compressive. As the soil stiffness decreases it provides less resistance to the abutment and piles causing larger tensile stresses. The wingwall pile is resisting some of the movement as well. The differential displacement between the wingwall and abutment piles ranged from 1 to 3 mm.

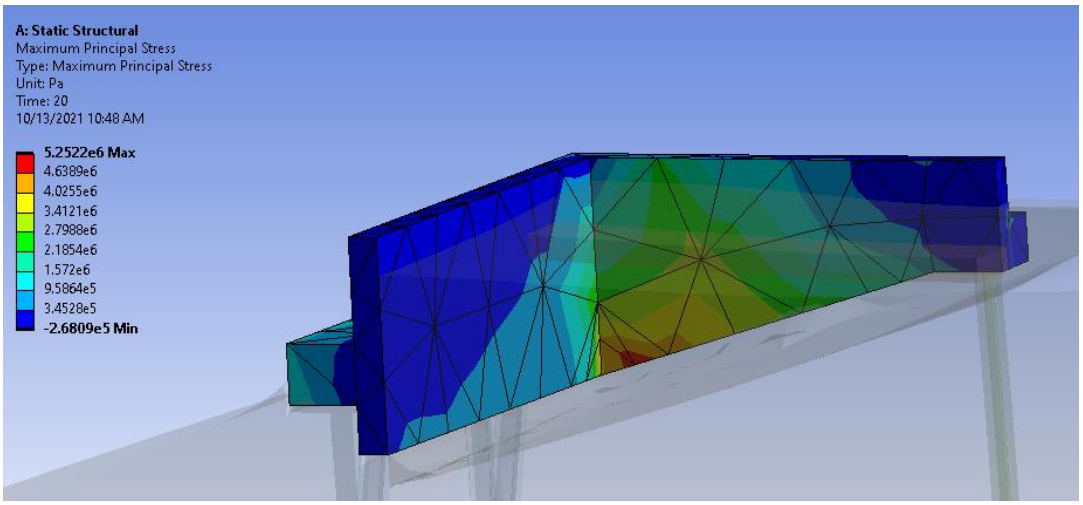

Figure 28. Stub Type Abutment - Maximum Principal Stress

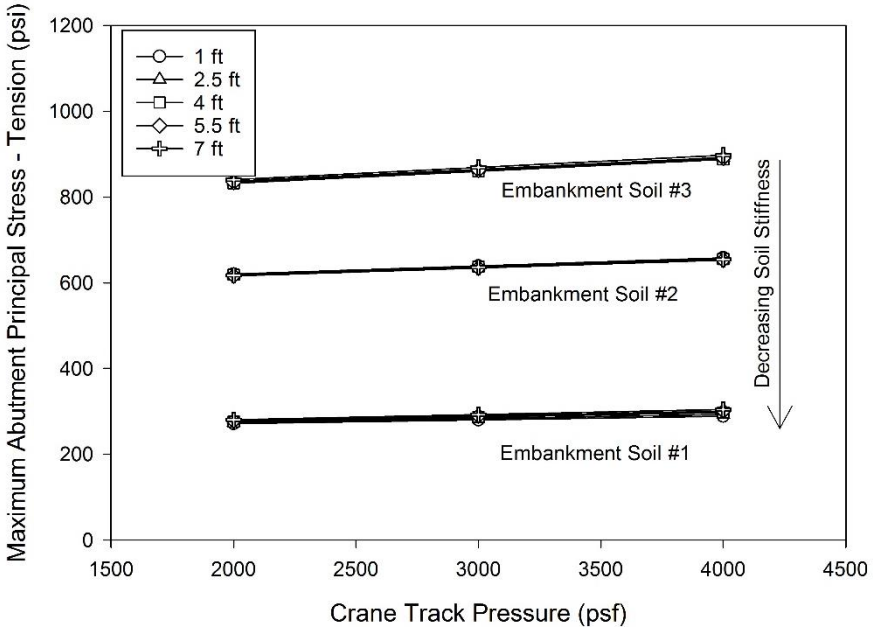

Figure 29. Full Height Abutment - Maximum Principal Stresses

An opposite trend was found for the full height abutment. The maximum principal tensile stress occurs at the interface of the pile cap and abutment for the full height abutment. The trend shown in Figure 29 agrees well with the maximum abutment displacement; Figure 17. As the soil stiffness increases the CLSM settles less and moves toward the full height abutment. The maximum principal stress isochrones for the full height abutment are shown in Figure 30.

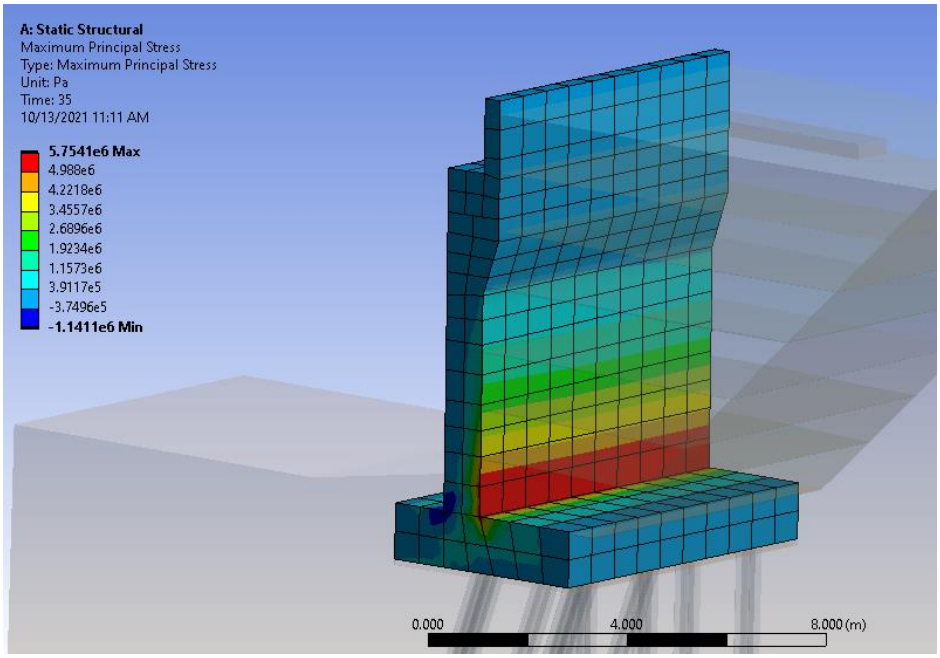

Figure 30. Full Height Abutment - Maximum Principal Stresses

The minimum abutment principal stresses from the analyses for the three abutments are shown in Figures 31, 32, and 33. The minimum principal stress for the stub type abutments increases as the soil stiffness decreases. The minimum principal stress was more sensitive when the soil stiffness is low. The minimum principal stress is also more sensitive to the position of the crane when the soil stiffness is low. The minimum principal stresses in the model are negative and represents compressive stress. Class

A concrete is required in the abutments. The minimum compressive strength of Class A concrete is 3,000 psi. The compressive strength of Class A concrete is much more than any of the compressive stresses found during the analysis.

In the stub type abutments, the minimum principal stress occurred near the pile connections. In the full height abutment, the minimum value occurred at the interface of the pile cap and abutment on the bridge side. This location is the opposite to the location of the maximum principal stress as can be seen in Figure 30.

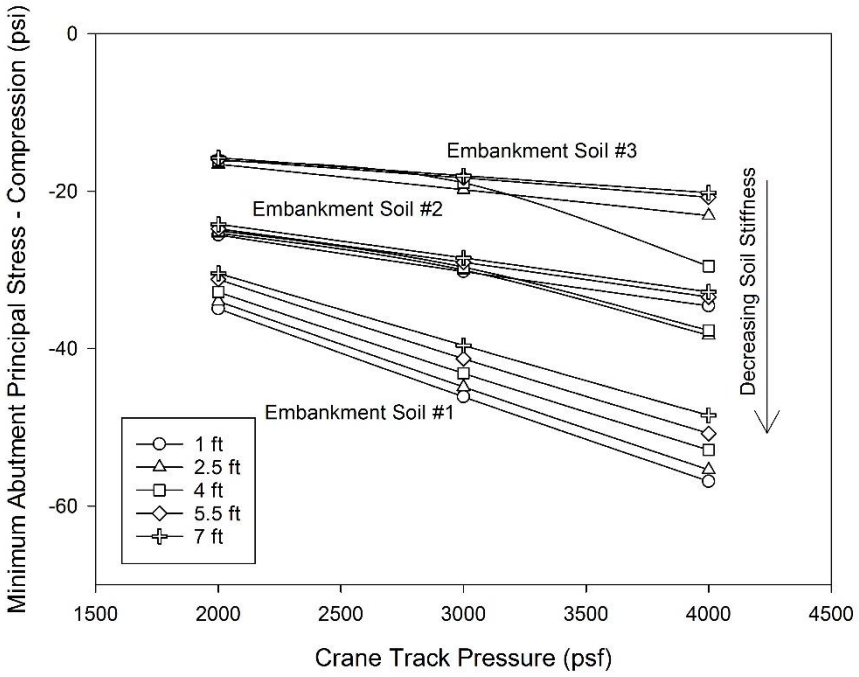

Figure 31. Type III Abutment - Minimum Principal Stresses

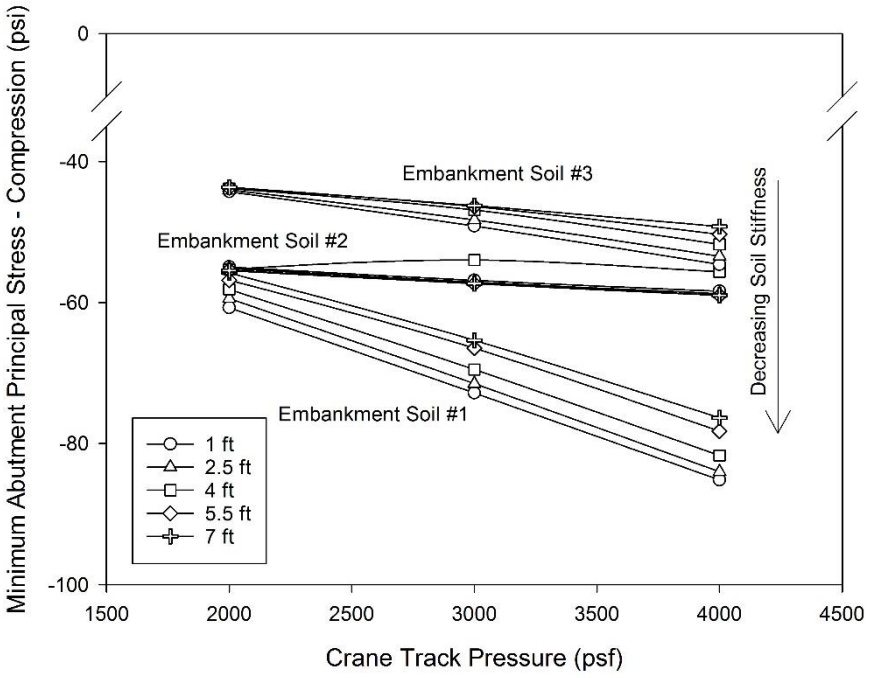

Figure 32. Type J Abutment - Minimum Principal Stresses

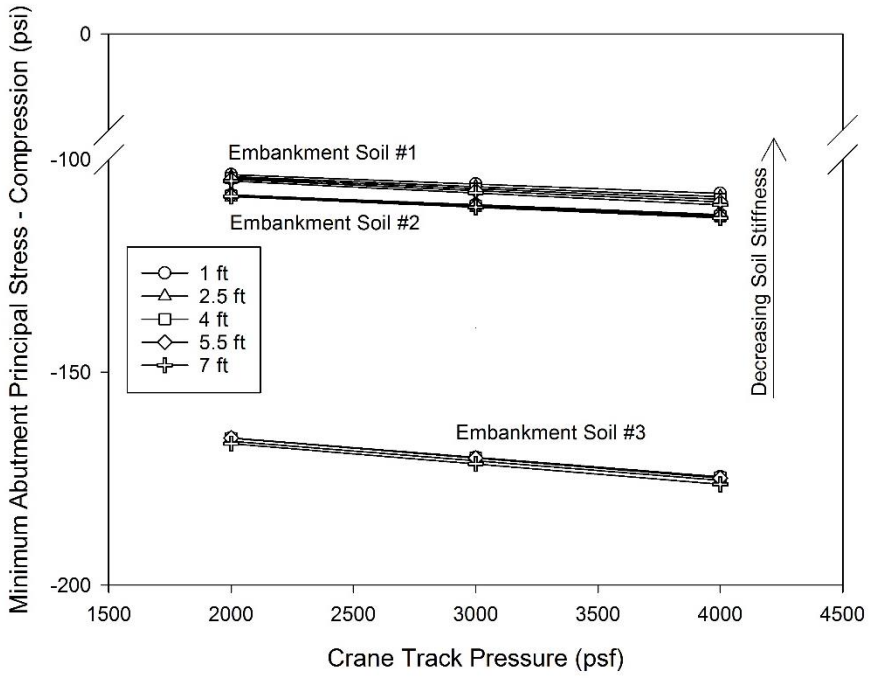

Figure 33. Full Height Abutment - Minimum Principal Stresses

The maximum abutment shear stresses from the analyses for the three abutments are shown in Figures 34, 36, and 38. For all the abutment types analyzed the maximum shear stress increases as the embankment soil decreases in stiffness. The effects of this are more noticable in the stub type abutments.

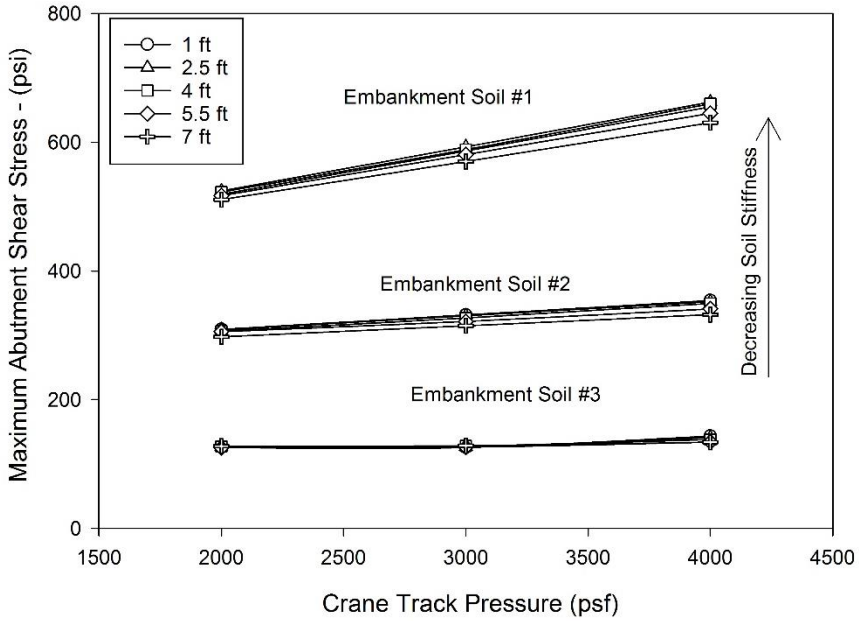

Figure 34. Type III Abutment - Maximum Shear Stresses

The maximum shear stress occurred at the centerline of the bridge seat and along the bottom edge of the wingwall for the Type III abutment. The location of the maximum shear stress is likely the result of a straight pile at that location. Isochrones of the shear stress distribution for the Type III abutment are shown in Figure 35. The maximum shear stress is represented by red in the figure.

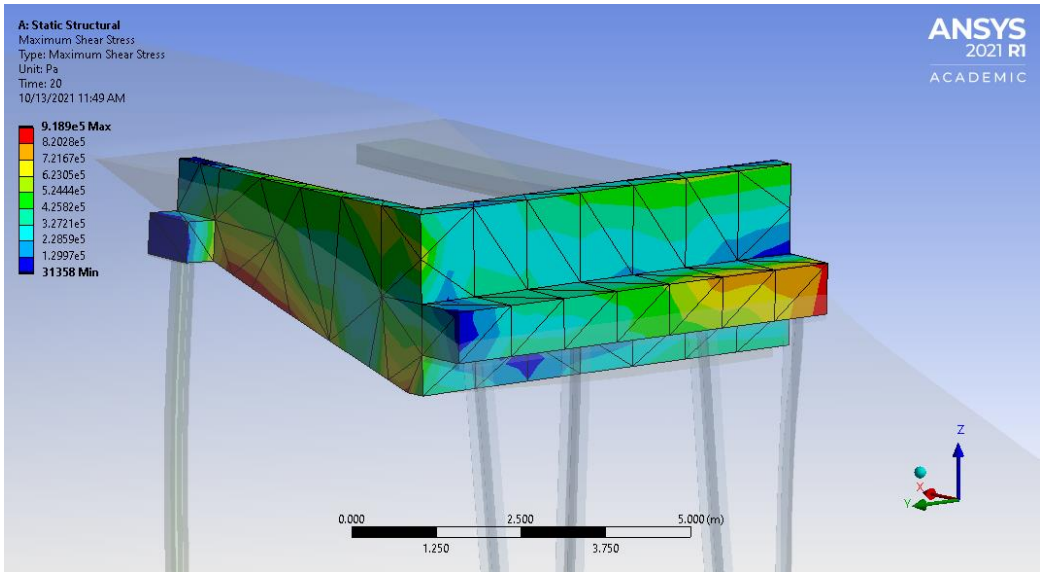

Figure 35. Type III Abutment – Shear Stress Isochrones

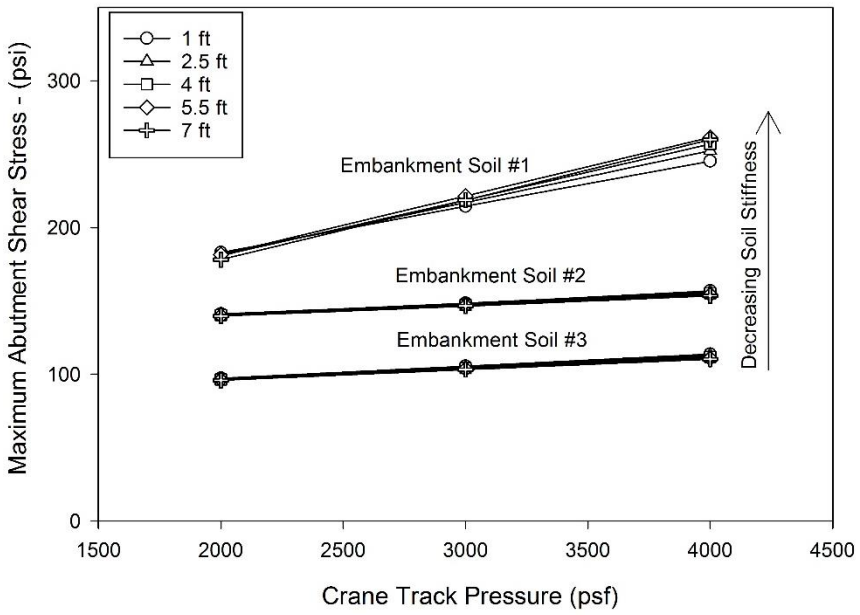

Figure 36. Type J Abutment - Maximum Shear Stresses

The maximum shear stress for the Type J abutment occurred along the inside face of the wingwall and abutment interface. The shear stress isochrones for the Type J abutment are shown in Figure 37. The abutment pile along the centerline of the

abutment for the Type J abutment is battered. The battered pile caused less shear stress in this area than the straight pile did for these analysis.

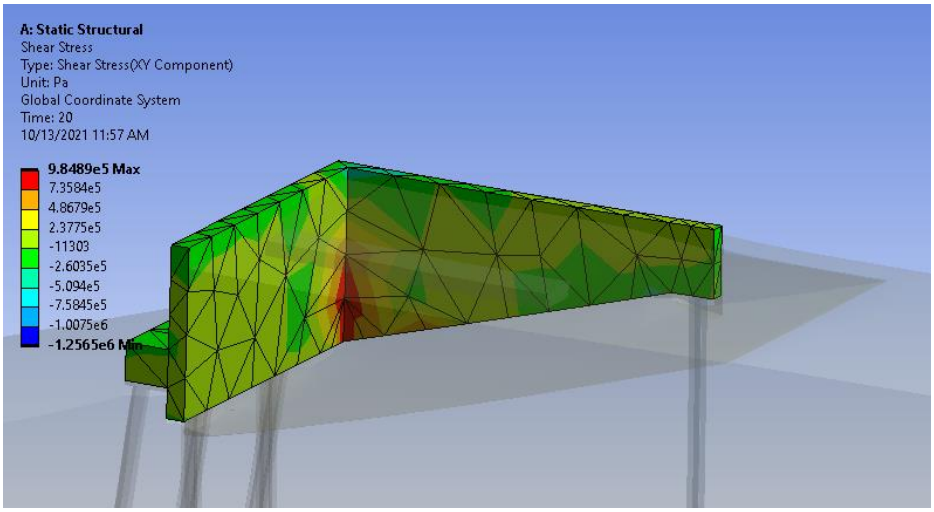

Figure 37. Type J Abutment - Shear Stress Isochrones

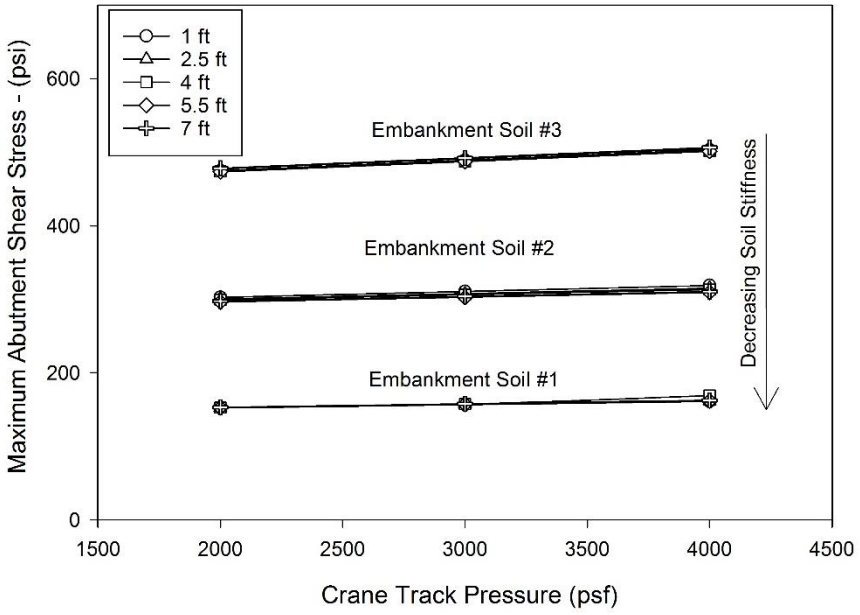

Figure 38. Full Height Abutment - Maximum Shear Stresses

The shear stresses for the full height abutment follow an opposite trend. As the soil stiffness increases the shear stresses also increase. This is due to the CLSM

pushing on the abutment as the soil stiffness increase. The maximum shear stress occurs near the bottom of the full height abutment. The shear stress isochrones are shown in Figure 39.

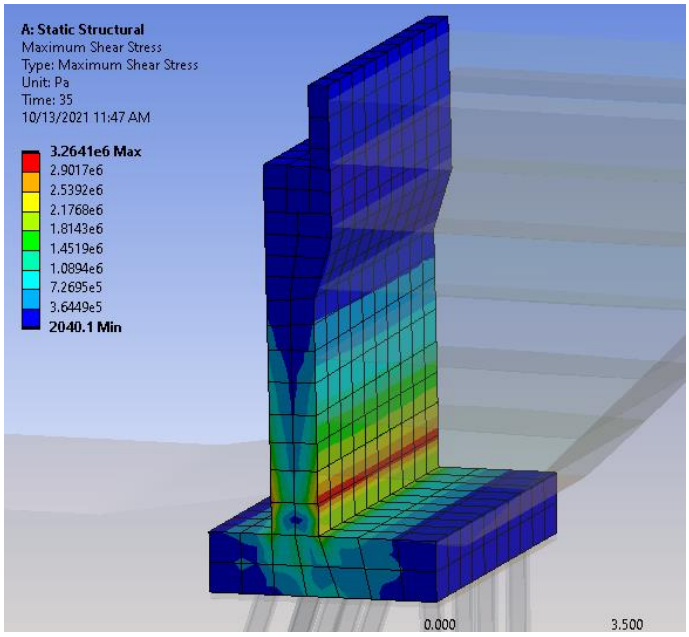

Figure 39. Full Height Abutment – Shear Stress Isochrones

4.2.2 On Granular Backfill

The response of the abutments to crane loading on granular backfill was studied in a limited capacity. Only one crane location and one crane pressure for each abutment design and soil was considered.

The maximum abutment displacements at the end of the simulation for each of the three abutments are shown in Figures 40. The soil stiffness is shown on the horizontal axis. The weakest soil is indicated by a 1.0 on the horizontal axis. The strongest soil is indicated by a 3.0 on the horizontal axis. The stub abutments experienced similar behavior. As the soil stiffness increased the maximum displacement of the abutment decreased. The full height abutment experienced the most movement

for soil 2. This phenomenon is like what was found when the backfill was CLSM. When the soil is weak the backfill will settle and rotate away from the abutment and, as modeled, will form a gap between the abutment and the backfill. If these gaps were to form during construction, they would likely be filled. There is not a process to fill gaps that form during an analysis within ANSYS.

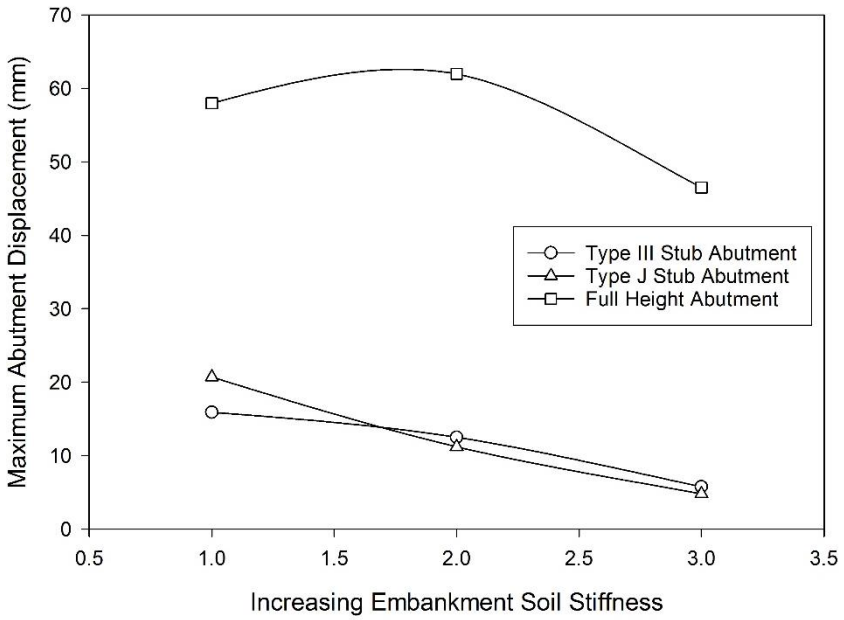

Figure 40. Granular Backfill – Abutment Displacements at End of Simulation

The maximum abutment pile displacements measured at the end of the simulations are shown in Figure 41. The pile displacements for the stub abutments match the abutment displacements well. This indicates that the abutments were not experiencing much tilting during the loading. The full height pile displacements do not match the top of the abutment movement. This indicates tilting of the abutment during loading.

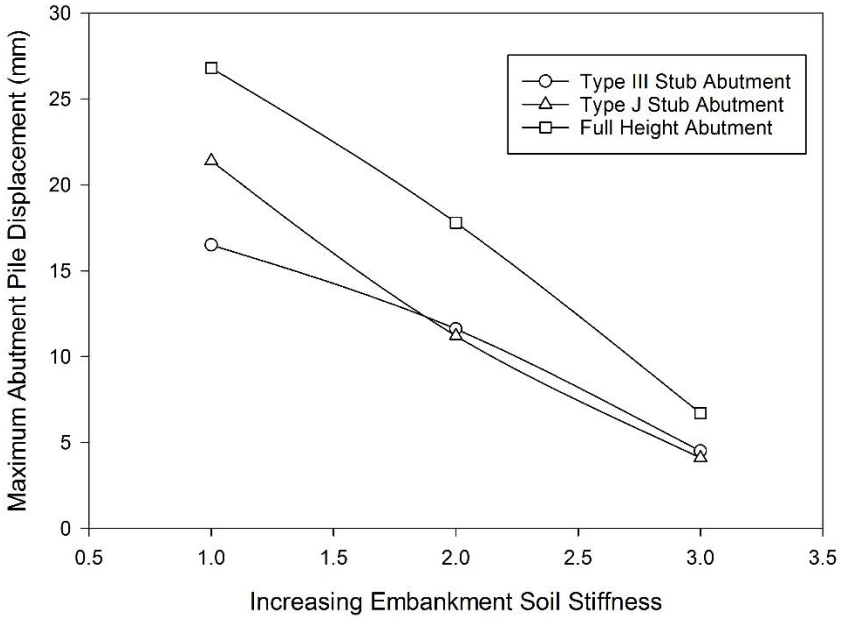

Figure 41. Granular Backfill - Maximum Pile Displacement

The maximum principal stresses in the abutment are shown in Figure 42. The stub abutments experienced a similar magnitude and trend for the maximum principal stress. The location of the maximum shear stress was like what was found when CLSM was used as backfill, Figure 28. The full height abutment experienced an opposite trend. This is likely due to the separation of backfill from the abutment.

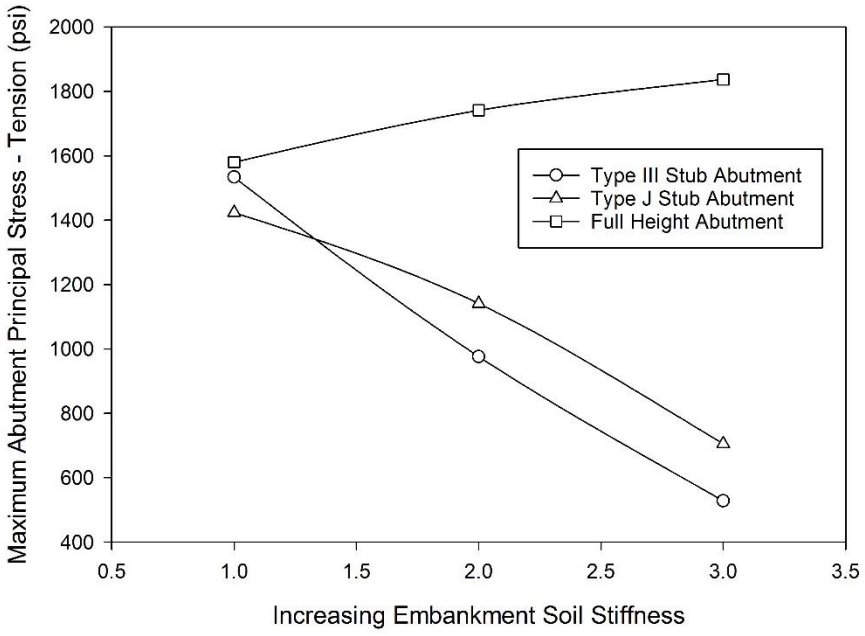

Figure 42. Granular Backfill – Abutment Maximum Principal Stresses

The minimum principal stresses recorded in the abutments are shown in Figure 43. The stub type abutments experience a similar trend. As the soil stiffness increases the compressive principal stress decreases. An opposite trend is found for the full height abutment.

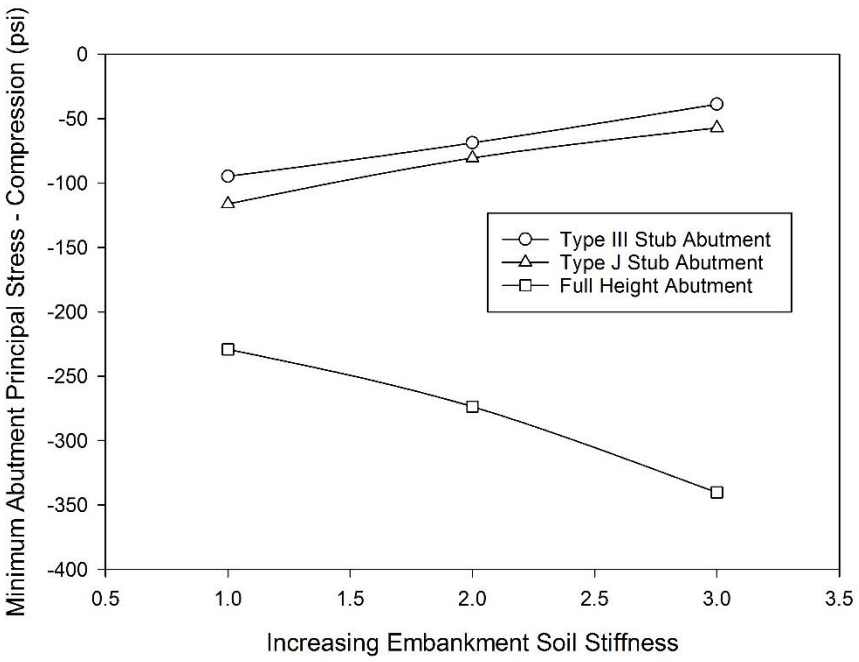

Figure 43. Granular Backfill – Abutment Minimum Principal Stresses

The maximum shear stresses in the abutment are shown in Figure 44. The stub abutments experienced similar behavior. As the soil stiffness increased the maximum shear stress decreased. The full height abutment experienced an opposite trend. The differences are the result of the backfill separating from the abutment.

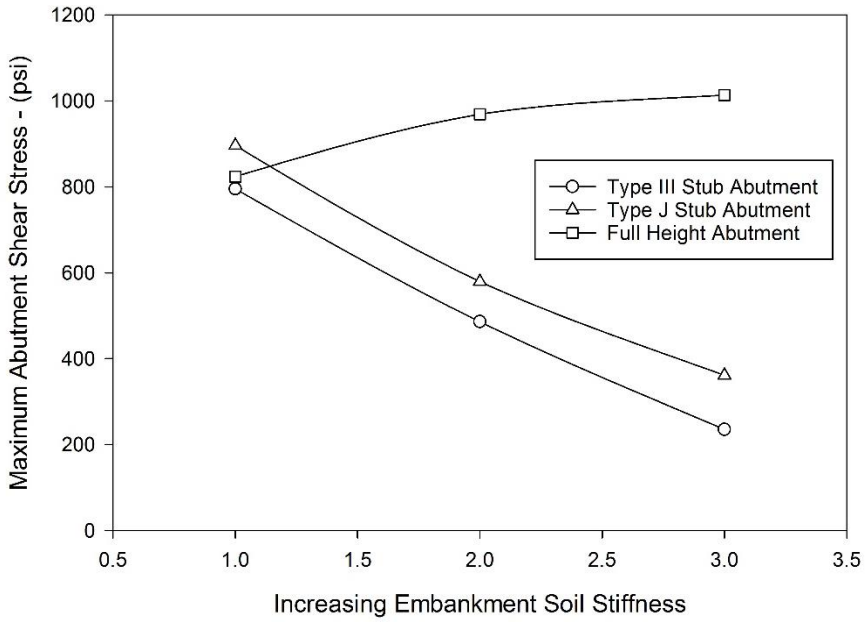

Figure 44. Granular Backfill - Abutment Maximum Shear Stresses

5.0 Conclusions

A parametric study was completed to investigate the impact of fluid CLSM placement and crane loading on bridge abutments. A limited study was completed to investigate granular backfill placement and crane loading on bridge abutments. Three abutment designs, three embankment soil stiffnesses, five crane positions, and three crane loadings were investigated. The parametric study results can be used to evaluate the influence of various parameters on the abutment behavior during backfill placement and crane loading. Through this study it was realized that the embankment soil has a much larger impact on the abutment behavior than the crane loading or position. A summary of the parametric study is below. The summary is separated into two parts. The first portion summarizes the behavior of the stub type abutments (Type III and Type J) while the second portion summarizes the full height abutment. A summary of the granular backfill study is included at the end.

Stub Type Abutments with CLSM Backfill

- As the embankment soil stiffness decreases the placement of fluid CLSM causes an increase in abutment displacement toward the bridge. The maximum abutment displacements at the end of CLSM placement for the worst embankment soil conditions were 12.1 mm for the Type III abutment and 20.7 mm for the Type J abutment.
- The abutment displacement increases as the soil stiffness decreases and the crane track pressure increases. The crane position with respect to the abutment backwall had a minor influence on the magnitude of the displacement for the Type III abutment. The influence of crane placement was larger for the Type J abutment. The maximum abutment displacements for the worst embankment soil conditions at the end of crane loading were 9.8 mm for the Type III abutment and 11.3 mm for the Type J abutment.
- The pile displacement under crane loading was similar to the abutment displacements. This suggest the abutment was not experiencing a large amount of tilting. The maximum pile displacements at the end of crane loading for the worst embankment soil conditions were 11 mm for the Type III abutment and 12.4 mm for the Type J abutment.
- During crane loading, as the soil stiffness decreased the maximum principal stress (tensile) increased. Similarly, when the soil stiffness decreased the minimum principal stress (compression) also increased.
- As the soil stiffness decreased the maximum shear stress increased in the abutment during crane loading.

Full Height Abutment with CLSM Backfill

- The soil stiffness did not have a large impact on the abutment response to fluid CLSM placement. The maximum abutment displacement during CLSM backfill placement was 15.3 mm for the full height abutment. Note, however, if CLSM fluid pressures are applied over the full height of the abutment, unacceptably large abutment displacements may occur. There is some evidence in the literature that suggest a gap may form between the abutment and underlying CLSM lifts allowing fluid pressures to develop over a larger height than that of the current fluid CLSM lift.
- During crane loading, when the soil stiffness is low the CLSM rotated away from the abutment resulting in minimal abutment displacement. As the soil stiffness increased the CLSM moved toward the abutment resulting in greater displacements for the abutment toward the bridge. The position of the crane and the crane track pressure had little impact on the displacement behavior. The maximum abutment displacement during crane loading was 20.4 mm for the full height abutment.
- The pile displacement was much less than the abutment top displacement during crane loading. This suggest the full height abutment was tilting away from the embankment. The maximum pile displacement during crane loading was 8.2 mm for the full height abutment.
- During crane loading, as the soil stiffness increased the maximum principal stress (tensile) increased. The maximum principal stress occurred at the intersection of the pile cap and the abutment. When the soil has a higher

stiffness the CLSM pushes toward the abutment causing it to tilt more resulting in larger principal stresses. A similar trend was observed for the minimum principal stress (compression).

- During crane loading, as the soil stiffness increased the maximum shear stress increased. This is a result of the movement described previously.

Granular Backfill

- Abutment movement during the placement of granular backfill using the flooding method was similar or more than what was found for CLSM backfill. This is especially noticeable for the full height abutment. The maximum abutment displacements during granular backfill placement was 13.2 mm for the Type III abutment, 21.3 mm for the Type J abutment, and 79 mm for the full height abutment.
- During crane loading, as soil stiffness increased the final abutment displacement decreased for the stub type abutments. The final abutment displacement initially increases and then decreases for the full height abutment. The maximum abutment displacements during crane loading were 15.9 mm for the Type III abutment, 20.7 mm for the Type J abutment, and 58 mm for the full height abutment
- During crane loading, as soil stiffness increased the maximum tensile stress, maximum compressive stress, and maximum shear stress decreased for the stub type abutments. An opposite trend was found for the full height abutment.

- When the soil is soft the granular backfill forms a gap with the full height abutment. This gap causes the abutment to essentially be isolated from the impacts of crane loading. As soil stiffness increases a gap does not form.

6.0 Recommendations

It is important to note that the analyses presented in this report are complex, involve many assumptions and are representative of the material, geometric, and loading parameters examined. The resulting displacements are reasonable and the analysis provided great insight, but the results should not be considered as representative of all situations involving such abutments and backfill materials. It is important to calibrate and validate the model predictions against real field measurements to improve confidence and minimize uncertainty.

The results of the simulation suggest that placement of CLSM before the placement of the superstructure may be feasible depending on the tolerable deformations. The behavior of the abutment is dependent on the embankment soil stiffness. Prior to fully implementing a new protocol further testing is suggested. Carefully monitored bridge abutments are suggested. The abutments would need to be instrumented and monitored during the placement of CLSM (or granular backfill) and while the girders are being set. Real time monitoring would allow the backfill placement or crane operations to be halted if the stresses or displacements became excessive. It is recommended that a stub type abutment be studied first.

The full height abutment is more difficult to study using the methods in this report. Full height abutments are designed on a project by project basis. The full height abutment presented in this report may not be representative of other full height abutments. Furthermore, the magnitude of movement for the full height abutment experienced may be deemed excessive despite the lift height being limited to 4 ft. As discussed, even if lift heights are 4 feet, there is limited evidence in the literature that

suggests it is possible for CLSM pressure to develop over larger portions of the wall height due to gapping.

Acknowledgements

The authors are grateful to ODOT for financial support of this project and for providing guidance for the work. We are particularly grateful to Walt Peters of ODOT for his support and guidance and for providing access to members of the bridge construction community. We also extend our thanks to Chris Harlin and Ladan Nelson of the ODOT Oklahoma City residency for providing CLSM samples. And to Matt Flusche and Raymond Flatt of Frontier Bridge for giving us the contractors perspective on cranes and crane loading.

References

Alizadeh, V., Helwany, S., Ghorbanpoor, A., & Oliva, M. (2014). Rapid-construction technique for bridge abutments using controlled low-strength materials. Journal of Performance of Constructed Facilities, 28(1), 149-156.

Alizadeh, V., Helwany, S., Ghorbanpoor, A., Oliva, M., & Ghaderi, R. (2015). CLSM bridge abutments–Finite element modeling and parametric study. Computers and Geotechnics, 64, 61-71.

Alizadeh, V. (2019). Finite element analysis of controlled low strength materials. Frontiers of Structural and Civil Engineering, 13(5), 1243-1250.

ANSYS. 2021. Ansys Mechanical User's Guide. Canonsburg, Pennsylvania.

Duncan, J. M., & Seed, R. B. (1986). Compaction-induced earth pressures under K 0-conditions. Journal of Geotechnical Engineering, 112(1), 1-22.

Newman, F.B., et al. CLSM Backfills for Bridge Abutments. Monroeville: GAI consultants, 1993.

Pons, F., Landwermeyer, J. S., & Kerns, L. (1998). Development of engineering properties for regular and quick-set flowable fill. In The design and application of controlled low-strength materials (flowable fill). ASTM International.

Schofield, A. N., and Wroth, P. 1968. *Critical state soil mechanics*. McGraw-hill London.

Schmitz, M. E., Parsons, R. L., Ramirez, G., & Zhao, Y. (2004). Use of controlled low-strength material as abutment backfill.

Shamsabadi, A., Khalili-Tehrani, P., Stewart, J. P., & Taciroglu, E. (2010a). Validated simulation models for lateral response of bridge abutments with typical backfills. Journal of Bridge Engineering, 15(3), 302-311.

Shamsabadi, A., & Kapuskar, M. (2010b). Nonlinear soil–abutment–foundation–structure interaction analysis of skewed bridges subjected to near-field ground motions. Transportation research record, 2202(1), 192-205.Snethen, D. R., & Benson, J. M. (1998). Construction of CLSM Approach Embankment to Minimize the Bump at the End of the Bridge. In The Design and Application of Controlled Low-Strength Materials (Flowable Fill). ASTM International.

Wilson, J. (1999). Flowable Fill as Backfill for Bridge Abutments. Report No. WI-16-99, Wisconsin Department of Transportation, Madison, Wisconsin.